ANALYSIS OF LUBRICATION GROOVE GEOMETRY

A Thesis presented to the Faculty of the Graduate School

University of Missouri-Columbia

In Partial Fulfillment

of the Requirements for the Degree

Master of Science

---

by

NOEL JOHN NORONHA

Dr. Noah D. Manring Thesis Supervisor

DECEMBER 2005

ACKNOWLEDGEMENTS

I would like to express my sincere appreciation and profound gratitude to my thesis advisor, Dr Noah D. Manring, for his continuous guidance, advice and encouragement throughout my graduate research. I would also like to extend my appreciation to Dr. Roger Fales and Dr. Steve C. Borgelt for serving on my thesis committee.

I would also like to thank the tremendous support given to me during my Masters from my family, friends and well wishers.

TABLE OF CONTENTS

LIST OF FIGURES

LIST OF TABLES

NOMENCLATURE

F	force
$\hat{F}$	dimensionless force
h_0	fluid film thickness
L_1	length from $x = 0$ till start of the groove
$\hat{L}_1$	dimensionless length
$\hat{L}_{1_0}$	dimensionless length at nominal condition
L_2	length from $x = 0$ till end of the groove
L_3	total length of the flat plate system
p_b	high pressure
p	characteristic pressure
Q	flow rate
$\hat{Q}$	dimensionless flow rate
$\hat{Q}_0$	dimensionless flow rate at nominal condition
Re	Reynolds number
T	torque
$\hat{T}$	dimensionless torque
u	velocity along x direction
U	sliding velocity
$\hat{U}$	dimensionless sliding velocity

v velocity along y direction

V squeeze film velocity

w width of the groove

$\hat{w}$ dimensionless width

$\hat{w}_0$ dimensionless width at nominal condition

ρ fluid density

σ normal stress

τ shear stress

μ coefficient of viscosity

δ depth of the groove

$\hat{\delta}$ dimensionless depth

$\hat{\delta}_0$ dimensionless depth at nominal condition

ANALYSIS OF LUBRICATION GROOVE GEOMETRY

Noel John Noronha

Dr. Noah D. Manring, Thesis Supervisor

ABSTRACT

Lubrication is process of using lubricants in moving machine components to reduce friction and wear between them and consequently to improve their running life. In this thesis, an analysis into the introduction of a groove in these components has been done and the various groove parameters that could influence better lubrication has been analyzed. The lubricating system considered in this thesis is a moving flat plate with a rectangular groove in it while its external housing is stationary. Equations that govern the flow rate, force and torque for this groove have been derived and the lubrication analysis has been done on these governing equations. Sensitivity analysis of flow, force and torque has been done taking into consideration two cases of the groove i.e. a short groove with deep depth and a long groove with shallow depth. Results are drawn from the values and plots obtained for the above cases. Based on the results obtained it is possible to determine the importance of each groove parameter in effective lubrication and to eliminate those which do not have any influence.

CHAPTER 1. INTRODUCTION

1.1 Introduction

Modern machinery has many moving parts that are in relative motion to each other. In these parts when one surface moves over the other, there is bound to be some resistance offered to its movement and the force that opposes this movement is called friction. Lubrication is simply the use of a material, which improves the smoothness of this surface-to-surface movement and the material that aids in this functioning is called a lubricant. Thus a lubricant is any substance that reduces friction and wear and provides smooth running and a satisfactory life for machine elements. Fluid film lubrication occurs when opposing bearing surfaces are completely separated by a lubricant film. The pressure generated within the fluid carries the applied load and the frictional resistance to motion arises entirely from the shearing of the viscous fluid. Friction F is proportional to the load W exerted by one surface on the other and its relation is given by

$$F = \text{constant x } W \tag{1.1}$$

The constant here is called the coefficient of friction (μ) and is dependent on the materials that are in sliding contact. Its value varies from 0.003 to 3.0 (Lansdown 2004). The coefficient of friction between two bodies is in fact not quite constant and varies with change in load and with sliding speed.

The way in which liquids lubricate can simply be explained by considering the example of a plain journal bearing as shown in Figure 1-1. As the shaft rotates in the bearing, lubricating oil is dragged into the loaded zone and the pressure and volume of the oil in the loaded zone both increase. The pressure rise and thickness of the oil film

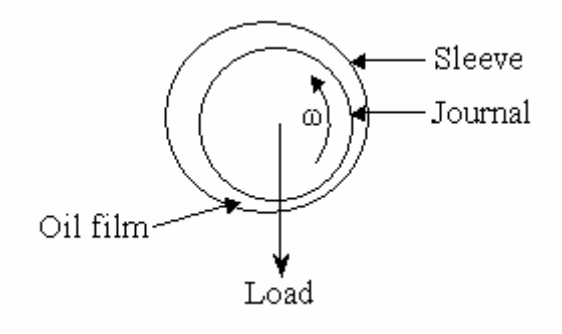

Figure 1-1. Plain journal bearing lubrication

will depend on the shaft speed and the lubricant viscosity. Lubrication that is achieved by the movement of a liquid is called hydrodynamic lubrication. In the case of the plain journal bearing, the rotation of the shaft causes lubricant to move into the loaded zone. Since the shaft and bearing surfaces come closer together in the loaded zone, the entry into this zone is tapered, like a curved wedge. A wedge is usually essential to produce hydrodynamic lubrication. In some cases a wedge may be generated on a perfectly flat slider because the center of the sliding face warms up in use and expands. When one bearing surface is moving towards the other, the lubricant between the two surfaces is squeezed and forced to move out of the space between them. The viscosity of the lubricant then tends to prevent the lubricant from being squeezed out. The oil film thickness depends on the speed of the bearing surfaces and on the oil viscosity (Lansdown 2004).

Hydrodynamic lubricated bearings depend upon the development of a thick film of lubricant between the journal and the sleeve so that the surface asperities do not make a contact through the fluid film. Since there is no contact in ideal hydrodynamic lubrication, the material properties of the journal and the sleeve become relatively

unimportant. The lubricant property of greatest importance in designing hydrodynamically lubricated bearings is the viscosity η, which is the measure of the internal shear resistance of the fluid. Figure 1-2 shows a layer of fluid interposed between a solid flat plate moving with steady velocity U and a fixed flat plate, where h is the lubricant film thickness (Collins 2003).

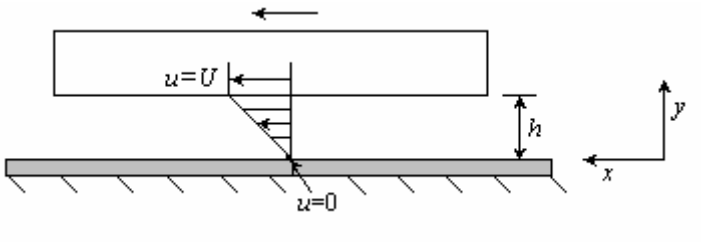

Figure 1-2. Illustration of linear velocity gradient across film thickness between parallel plates.

In this thesis an analysis will be conducted on the lubrication effects on a flat plate having a groove and moving with velocity U with respect to a stationary plate. The pressure variation along the length of the plate and also the influence of the flow rate, total force and torque effects on the flat plate system will be determined. The goal of the project is to analyze the parameters of dependence of the flat plate and its individual effects on the lubrication phenomenon. Important conclusions will be drawn at the end from the results obtained. The potential applications of this research is mainly in pumps like axial piston pumps where the grooves are placed on the piston thus aiding in lubrication by preventing the piston from coming in contact with the housing during longitudinal motion. They are also used in valves like spool valves where the grooves are etched in the housing and thus preventing the spool from causing friction due to contact.

1.2 Literature Review

Blatter et al., (1998) have made an attempt to improve localized liquid lubrication of flat surface with laser written fine grooves on the sliding part with the idea that this groove would serve as a reservoir to increase the quantity of the lubricant and also keeping the lubricant in the desired place. The work was done for sliding contacts in performance of micromechanical assemblies like watches. A special laser technique was employed to produce microscopic patterns on a highly polished single crystal sapphire flat that was completely covered in the lubricant Moebius 941. A polished steel ball was pressed onto the rotating sapphire disks. The results showed much longer sliding life of the flat that indicated the grooves storing the lubricant and replenishing the track with fresh oil. It was concluded that wear can be reduced and sliding life significantly extended by appropriate size and form of the micropattern with the possibility of having virtually no wear and unlimited sliding with fine grooves.

The use of micro pattern/pores on parallel mating sliding surfaces to show that surface texturing can efficiently improve hydrodynamic lubrication on reciprocating automotive components has been shown by Ronen et al., (2001). Microstructure plays an important role in friction control because of its effect on the build up of hydrodynamic fluid film between the mating surfaces. Increasing the number of pores along the axial length of the system reduces friction sharply. Experiments showed that there was friction reduction in surface texturing as compared to non-textured surfaces, which was seen to be higher than 28%.

Similar work on micro-patterned surfaces on the load carrying capacity using Computational Fluid Dynamics (CFD) was carried out by Sahlin et al., (2005). The

hydrodynamic performance in terms of friction force and load carrying capacity and its dependence on groove geometry and flow conditions was analyzed using CFD. For the CFD model the Navier-Stokes equations were solved considering constant viscosity and density, assuming steady state conditions in x and y directions. The results showed an increase in the pressure build-up in the groove with the value of Reynolds number and the normal force increases with increasing groove width. A certain maximum groove depth exists where an increase does not lead to further increase in load carrying capacity. The authors concluded that an introduction of a micro-groove on one of the parallel surfaces affects the flow and pressure pattern, giving a net pressure build up and load carrying capacity on the film. It was also seen that friction forces decreases with increasing values of groove depth and width.

Ivantysynova and Huang (2002) have worked on the design of the lubricating gaps of displacement machines where the gap height changes with operating parameters (pressure, speed, viscosity etc) and the gap flow condition is mainly influenced by this height. The axial and reaction force causes the piston in the system to be inclined which creates a wedge and thus develops a pressure field inside the gap due to the hydrodynamic effect. The gap geometry strongly influences the volumetric and friction losses (influence of surface roughness is neglected here relative to gap height), thus affecting the system efficiency. A new piston contour has been analyzed comparative to a conventional cylindrical form. Simulations were carried on macro (gap shape variations) and micro (quality/roughness of sliding surfaces) geometry to calculate the flow velocity field, load bearing and hydrodynamic pressure field in the lubricating gaps. The results show that this contour improves the pressure field as well as leads to gaps heights above a

critical value of 1μm allowing viscous friction. However further investigations analyzing all aspects of this new contour is to be examined.

Research on the lubricant spreading characteristics based on its molecular weight in groove shaped textures has been done by Zhang et al., (2003). The experiment included investigating the effect of nano textures (perfectly rectangular) on lubricant spreading in a commercially available CD-RW and results showed that lubricant spreading regions become smaller as molecular weight increases which indicates that the larger the molecular weight, slower the lubricant spread. Findings show that increasing the groove depth, aids in lubricant spreading and weakens the molecular weight dependence. The paper also mentions of the surface energy characteristics of a material, where at high surface energy, intermolecular interaction becomes less significant and the dependence of lubricant spreading on molecular weight weakens. Similar work on the lubricant spreading characteristics in minute grooves using experiments and Monte Carlo simulations has been done by Zhang et al., (2002), the results prove that lubricant spreading becomes slower as molecular weight increases.

Determining the pressure distribution over a square edged rectangular groove was worked on by Hargreaves and Elgezawy (1998), where pressures were calculated at every mesh point using the Reynolds equation i.e. a finite difference mesh set up over the complete bearing surface, including the groove. Experimental pressure profiles along and across a transverse groove machined on an inclined flat slider pad and also a theoretical model to predict these pressures were developed. The loss factor that accounts for lubricant inertia as the lubricant enters the sudden expansion (bearing land to groove) and the sudden contraction (groove to bearing land) was calculated for each mesh point

across the groove. This loss factor modified the pressure calculation from the Reynolds equation. Results show good correlation between predicted and measured pressure profiles for a variety of operating conditions like relative sliding velocity, angle of inclination of the pad, groove width, groove depth etc.

Costa et al., (2000) have studied the influence of groove location and supply pressure on the performance of a steadily loaded journal bearing with a single-axial groove. A test apparatus was set up which consisted of the test bearing, the shaft driving system and the loading device and various measurement devices for torque, oil, temperature, pressure etc were connected to this test device. The angular location of the groove was changed from $\phi = -30$ degrees to $\phi = +30$ degrees in relation to the load line. The test results showed that for $\phi = -30$ degrees, the hydrodynamic pressure was at its maximum with also an increase in friction torque while there was a reduction observed for both oil flow rate and shaft temperature. For $\phi = +30$, a reduction in maximum temperature and friction torque and a moderate increase in oil flow rate and maximum hydrodynamic pressure was seen. For all values of applied load and all groove locations, oil flow rate increased significantly with increasing supply pressure.

A numerical model to study the effects of groove geometry on the hydrodynamic lubrication mechanism of thrust washers was developed by Yu et al., (2001). The model investigated the effects of radial groove width, depth, shape, number of grooves and operating conditions on pressure distribution, lubricant film thickness, flow rate and frictional torque. The model consisted of a smooth lower disk with grooves while the upper disk rotates with a constant angular velocity and is ungrooved. The results indicated that shallow and wide grooves could support significant loads and develop

sufficient film thickness to prevent the mating surfaces from coming in contact and that an optimum groove number exists which supports a maximum load. However as the groove number increases beyond a certain limit the load capacity decreases. A groove depth of the order of minimum film thickness is necessary to establish hydrodynamic pressure. The results also show that trapezoidal groove shape supports more load than either round or triangular shaped grooves when the groove depth ratio is small and when the ratio is large, the triangular groove supports more load. Torque decreases as groove number increases, which is mainly due to the increase in the average film thickness provided by the increased groove portion in the pad.

1.3 Research Objective

The papers in the literature review have covered the influence of microgrooves on system surfaces, lubricating gaps on displacement machines and effect of molecular weights in lubricating spreading in grooves. Also the papers included the pressure distribution on grooves and influence of groove location and geometry. The objective of this thesis is to determine the effects of a groove on lubrication in a simple flat plate system. The various factors affecting the system will be individually analyzed and the importance of each parameter in assisting the lubrication will be presented. The effect of the groove size, depth and location for different cases of sliding velocity of the flat plate will also be analyzed. The analysis is carried out in the non-dimensional form, which helps in scaling factors, and also that engineers prefer equations in non-dimensional form. However the final results are converted back and shown in its dimensional form. Sensitivity analysis of flow rate, force and torque are done during this project, which was

not seen in other research papers during literature review. Suitable and important conclusions based on the results obtained and prospects for future work will be made at the end.

1.4 Thesis Outline

The thesis report is complied of four chapters. The first chapter gives a basic introduction of lubrication and some of its properties and also the influence of lubrication in bearings. A brief literature survey of the similar work already done in this area is shown and finally the research objective of this thesis is outlined.

The bulk and the most important part of this thesis is Chapter 2 that analyzes the flat plate system considered in this project. Here the two dimensional Navier Stokes Equation is used to derive the governing equation of motion for the fluid and subsequently the volumetric flow rate through a flat plate. This equation also gives the pressure differential along the length of the system, which is then non-dimensionalized to analyze its individual terms. Analysis of pressure along the length of the flat plate with a groove in it and also flow, force and torque analysis of the system is made. To pick out the influence of individual parameters on the lubrication effects of a flat plate system, sensitivity analysis is done to get the equations of the volumetric flow rate, force and torque. At the end of the chapter, these equations are converted back into its dimensional form.

In Chapter 3, the equations derived in the previous chapter are studied in detail. To broaden the results scenario, two cases of groove size are considered. Grooves with deep depth and short width and grooves with shallow depth and long width were

considered. Sensitivity results of volumetric flow rate, force and torque for these two groove cases are obtained for different sliding velocities U. The results are tabulated and also plotted for better understanding. Each plot of the sensitivity and tables are then individually analyzed for understanding the importance of each parameter affecting the systems flow rate, force and torque.

Chapter 4 reports the conclusion of this thesis. Based on the results obtained in Chapter 3, each groove case is analyzed and suitable and important assumptions are made. Scope for future work in this area is also presented in this chapter.

CHAPTER 2. ANALYSIS

2.1 Introduction

This chapter is devoted to the development of the governing equations for the lubrication problem that will be studied in this thesis. To analyze the lubrication conditions, the equation for conservation of mass and conservation of momentum for a low-Reynolds-number flow is used. The Reynolds equation will then be non-dimensionalized so that the individual terms in the equation can be analyzed. This form will then be applied to analyze the model considered and various conclusions will be derived based on the results obtained. Also, several designs and operating conditions are taken into consideration during the analysis process and the conclusions are based on the best performance characteristics of either one or of all the cases combined.

2.2 Lubrication Geometry

The model for the lubrication analysis is shown in Figure 2-1. The system has been divided into three segments 1, 2 and 3 with lengths L_1, L_2 and L_3. It has a groove of depth δ and width w. The flat plate moves with sliding velocity U in the positive x-direction and has squeeze film velocity V in the positive y-direction. The system is two dimensional along coordinates x and y for the analysis, with a gap h_0 between the flat plate and its housing. This gap describes the lubricating film thickness between the two flat surfaces and is of the order of 25μm (about half the thickness of a human hair). The pressure varies along the positive x direction and this will be analyzed to describe the flow rate Q, force F and torque T acting on the system.

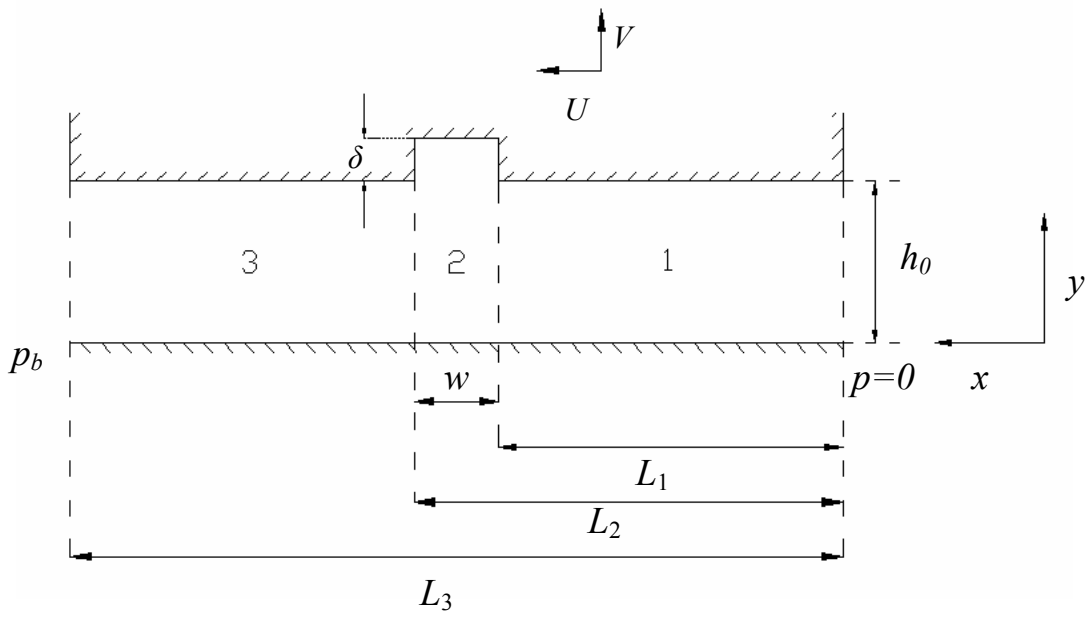

Figure 2-1. Straight flat plate with groove depth δ.

2.3 Governing Equation

Navier-Stokes equations are the fundamental partial differential equations that describe the flow of incompressible fluids. For incompressible fluids, density remains constant. In this section, the Navier-Stokes equations that are the classical governing equations that govern the dynamics of fluid motion, are derived, (Fox and McDonald 1985). The differential equations of motion along x and y components are given by

$$\rho g_x + \frac{\partial \sigma_{xx}}{\partial x} + \frac{\partial \tau_{yx}}{\partial y} = \rho\left(\frac{\partial u}{\partial t} + u\frac{\partial u}{\partial x} + v\frac{\partial u}{\partial y}\right) \tag{2.1}$$

$$\rho g_y + \frac{\partial \sigma_{yy}}{\partial y} + \frac{\partial \tau_{xy}}{\partial x} = \rho\left(\frac{\partial v}{\partial t} + u\frac{\partial v}{\partial x} + v\frac{\partial v}{\partial y}\right) \tag{2.2}$$

where ρ is the fluid density, u and v are velocity components in x and y directions respectively, σ_{xx}, σ_{yy}, τ_{yx}, τ_{xy} are the stresses along these coordinates. Equations (2.1)

and (2.2) are the differential equations of motion for any fluid satisfying the continuum assumption, i.e. the fluid is treated as an infinitely divisible substance and we are not concerned with the behavior of its individual molecules. For Newtonian fluid, the viscous stress is proportional to the rate of shearing strain. The stresses may be expressed in terms of velocity gradients and fluid properties in rectangular coordinates as follows:

$$\tau_{xy} = \tau_{yx} = \mu\left(\frac{\partial u}{\partial y} + \frac{\partial v}{\partial x}\right) \tag{2.3}$$

$$\sigma_{xx} = -p + 2\mu\frac{\partial u}{\partial x} - \frac{2}{3}\mu\left(\frac{\partial u}{\partial x} + \frac{\partial v}{\partial y}\right) \tag{2.4}$$

$$\sigma_{yy} = -p + 2\mu\frac{\partial v}{\partial y} - \frac{2}{3}\mu\left(\frac{\partial u}{\partial x} + \frac{\partial v}{\partial y}\right) \tag{2.5}$$

where μ is the coefficient of viscosity of the fluid, p is the local thermodynamic pressure. If these expressions are introduced into the differential equations of motion i.e. Equations. (2.1) and (2.2), the resulting expressions are

$$\rho g_x + \frac{\partial}{\partial x}\left[-p + 2\mu\frac{\partial u}{\partial x} - \frac{2}{3}\mu\left(\frac{\partial u}{\partial x} + \frac{\partial v}{\partial y}\right)\right] + \frac{\partial}{\partial y}\left[\mu\left(\frac{\partial u}{\partial y} + \frac{\partial v}{\partial x}\right)\right] = \rho\left(\frac{\partial u}{\partial t} + u\frac{\partial u}{\partial x} + v\frac{\partial u}{\partial y}\right) \tag{2.6}$$

$$\rho g_y + \frac{\partial}{\partial y}\left[-p + 2\mu\frac{\partial v}{\partial y} - \frac{2}{3}\mu\left(\frac{\partial u}{\partial x} + \frac{\partial v}{\partial y}\right)\right] + \frac{\partial}{\partial y}\left[\mu\left(\frac{\partial u}{\partial y} + \frac{\partial v}{\partial x}\right)\right] = \rho\left(\frac{\partial v}{\partial t} + u\frac{\partial v}{\partial x} + v\frac{\partial v}{\partial y}\right) \tag{2.7}$$

These equations of motion are called the Navier-Stokes equations and are greatly simplified when applied to incompressible flows in which variations in fluid viscosity can be neglected. Under these conditions the Equations (2.6) and (2.7) reduce to

$$\rho\left(\frac{\partial u}{\partial t}+u\frac{\partial u}{\partial x}+v\frac{\partial u}{\partial y}\right)=\rho g_x-\frac{\partial p}{\partial x}+\mu\left(\frac{\partial^2 u}{\partial x^2}+\frac{\partial^2 u}{\partial y^2}\right) \tag{2.8}$$

$$\rho\left(\frac{\partial v}{\partial t}+u\frac{\partial v}{\partial x}+v\frac{\partial v}{\partial y}\right)=\rho g_y-\frac{\partial p}{\partial y}+\mu\left(\frac{\partial^2 v}{\partial x^2}+\frac{\partial^2 v}{\partial y^2}\right) \tag{2.9}$$

Let forces ρg_x and ρg_y be written as f_x and f_y respectively. Since there are potentially different scales of phenomenon occurring within the flow field, it is useful to write the Navier-Stokes equations in non-dimensional form. To do this we introduce the following definitions:

$$\begin{gathered} u=\hat{u}U\ ,\ v=\hat{v}V\ ,\ t=\hat{t}\tau\ ,\ f_x=\hat{f}_xF_x\ , \\ f_y=\hat{f}_yF_y\quad p=\hat{p}p_b\ ,\ x=\hat{x}\,L_3\ ,\ \mathrm{y}=\hat{y}\,L_3 \end{gathered} \tag{2.10}$$

where the carets denote the dimensionless quantities. Here τ is a quantity of time that is typical of some transient behavior within the flow, F_x and F_y is a characteristic force acting on the fluid, p is a characteristic pressure of the fluid. Substituting Equation (2.10) into Equations (2.8) and (2.9) yields the following dimensionless results for the Navier-Stokes equations:

$$\begin{gathered} \left(\frac{\rho L_3^{\,2}}{\mu\tau}\right)\frac{\partial\hat{u}}{\partial\hat{t}}+\left(\frac{\rho UL_3}{\mu}\right)\hat{u}\frac{\partial\hat{u}}{\partial\hat{x}}+\left(\frac{\rho VL_3}{\mu}\right)\hat{v}\frac{\partial\hat{u}}{\partial\hat{y}}= \\ \frac{F_xL_3^{\,2}}{\mu U}\hat{f}_x-\left(\frac{p_bL_3}{\mu U}\right)\frac{\partial\hat{p}}{\partial\hat{x}}+\left(\frac{\partial^2\hat{u}}{\partial\hat{x}^2}+\frac{\partial^2\hat{u}}{\partial\hat{y}^2}\right) \end{gathered} \tag{2.11}$$

$$\begin{gathered} \left(\frac{\rho L_3^{\,2}}{\mu\tau}\right)\frac{\partial\hat{v}}{\partial\hat{t}}+\left(\frac{\rho UL_3}{\mu}\right)\hat{u}\frac{\partial\hat{v}}{\partial\hat{x}}+\left(\frac{\rho VL_3}{\mu}\right)\hat{v}\frac{\partial\hat{v}}{\partial\hat{y}}= \\ \frac{F_yL_3^{\,2}}{\mu V}\hat{f}_y-\left(\frac{p_bL_3}{\mu V}\right)\frac{\partial\hat{p}}{\partial\hat{y}}+\left(\frac{\partial^2\hat{v}}{\partial\hat{x}^2}+\frac{\partial^2\hat{v}}{\partial\hat{y}^2}\right) \end{gathered} \tag{2.12}$$

For steady flow, in the absence of body forces, the Navier-Stokes Equations (2.11) and (2.12) reduce to the following form:

$$\left(\frac{\rho U L_3}{\mu}\right)\hat{u}\frac{\partial \hat{u}}{\partial \hat{x}}+\left(\frac{\rho V L_3}{\mu}\right)\hat{v}\frac{\partial \hat{u}}{\partial \hat{y}}=-\left(\frac{p_b L_3}{\mu U}\right)\frac{\partial \hat{p}}{\partial \hat{x}}+\left(\frac{\partial^2 \hat{u}}{\partial \hat{x}^2}+\frac{\partial^2 \hat{u}}{\partial \hat{y}^2}\right) \tag{2.13}$$

$$\left(\frac{\rho U L_3}{\mu}\right)\hat{u}\frac{\partial \hat{v}}{\partial \hat{x}}+\left(\frac{\rho V L_3}{\mu}\right)\hat{v}\frac{\partial \hat{v}}{\partial \hat{y}}=-\left(\frac{p_b L_3}{\mu V}\right)\frac{\partial \hat{p}}{\partial \hat{y}}+\left(\frac{\partial^2 \hat{v}}{\partial \hat{x}^2}+\frac{\partial^2 \hat{v}}{\partial \hat{y}^2}\right) \tag{2.14}$$

Equations (2.13) and (2.14) can be written as

$$\mathrm{Re}_x\,\hat{u}\frac{\partial \hat{u}}{\partial \hat{x}}+\mathrm{Re}_y\,\hat{v}\frac{\partial \hat{u}}{\partial \hat{y}}=-\left(\frac{p_b L_3}{\mu U}\right)\frac{\partial \hat{p}}{\partial \hat{x}}+\left(\frac{\partial^2 \hat{u}}{\partial \hat{x}^2}+\frac{\partial^2 \hat{u}}{\partial \hat{y}^2}\right) \tag{2.15}$$

$$\mathrm{Re}_x\,\hat{u}\frac{\partial \hat{v}}{\partial \hat{x}}+\mathrm{Re}_y\,\hat{v}\frac{\partial \hat{v}}{\partial \hat{y}}=-\left(\frac{p_b L_3}{\mu V}\right)\frac{\partial \hat{p}}{\partial \hat{y}}+\left(\frac{\partial^2 \hat{v}}{\partial \hat{x}^2}+\frac{\partial^2 \hat{v}}{\partial \hat{y}^2}\right) \tag{2.16}$$

where Re_x and Re_y is the Reynolds number in the *x* and *y* directions and is given by

$$\mathrm{Re}_x=\frac{\rho U L_3}{\mu} \tag{2.17}$$

$$\mathrm{Re}_y=\frac{\rho V L_3}{\mu} \tag{2.18}$$

For low Reynolds number flow, the Reynolds number must be much less than unity. Under such conditions, it can be seen from Equations (2.15) and (2.16), that Re_x and Re_y □ $\frac{p_b L_3}{\mu U}$ and $\frac{p_b L_3}{\mu V}$. Then the governing equation of motion for the fluid is given by

$$\left(\frac{p_b L_3}{\mu U}\right)\frac{\partial \hat{p}}{\partial \hat{x}}=\left(\frac{\partial^2 \hat{u}}{\partial \hat{x}^2}+\frac{\partial^2 \hat{u}}{\partial \hat{y}^2}\right) \tag{2.19}$$

$$\left(\frac{p_b L_3}{\mu V}\right)\frac{\partial \hat{p}}{\partial \hat{y}}=\left(\frac{\partial^2 \hat{v}}{\partial \hat{x}^2}+\frac{\partial^2 \hat{v}}{\partial \hat{y}^2}\right) \tag{2.20}$$

In dimensional form, this result is written as

$$\mu\left(\frac{\partial^2 u}{\partial x^2}+\frac{\partial^2 u}{\partial y^2}\right)=\frac{\partial p}{\partial x} \tag{2.21}$$

$$\mu\left(\frac{\partial^2 v}{\partial x^2}+\frac{\partial^2 v}{\partial y^2}\right)=\frac{\partial p}{\partial y} \tag{2.22}$$

Since v is small compared to u i.e. $u \gg v$, it can be assumed that v is insignificant and $\frac{\partial p}{\partial x} \gg \frac{\partial p}{\partial y}$. Thus Equation (2.22) can be dropped from the analysis. If a one-dimensional flow field is considered where the pressure varies only in the x direction (the direction of flow) and the velocity varies only in the y direction (normal to the direction of flow), Equation (2.21) may be written more explicitly as (Manring 2005).

$$\mu\frac{d^2 u}{dy^2}=\frac{dp}{dx} \tag{2.23}$$

Integrating and solving for u in Equation (2.23)

$$u=\frac{1}{2\mu}\frac{\partial p}{\partial x}y^2+D_1 y+D_2 \tag{2.24}$$

Where D_1 and D_2 are the constants of integration. Applying the boundary conditions $u(0)=0$ and $u(h)=U$ into Equation (2.24), then

$$D_2=0 \tag{2.25}$$

$$D_1=\frac{1}{h}\left(U-\frac{1}{2\mu}\frac{\partial p}{\partial x}h^2\right) \tag{2.26}$$

Substituting D_1 and D_2 back in Equation (2.24) and rearranging

$$u=-\frac{1}{2\mu}\frac{\partial p}{\partial x}(h-y)y+U\frac{y}{h} \tag{2.27}$$

Using this result, the volumetric flow rate in the x direction is written as

$$Q = \int_0^h u\partial y = \underbrace{-\frac{1}{12\mu}\frac{\partial p}{\partial x}h^3}_{\text{Poiseuille flow}} + \underbrace{U\frac{h}{2}}_{\text{Couette flow}} \tag{2.28}$$

Steady, incompressible, viscous flow through a channel with flat parallel walls is called the Poiseuille flow and its velocity distribution is usually parabolic. The term Couette flow traditionally denotes a uni-directional, non-rotating flow confined between two plates, of which one is moving with constant velocity. Its velocity profile is usually linear. Equation (2.28) can be rearranged as

$$\frac{\partial p}{\partial x} = 12\mu\left(\frac{U}{2h^2} - \frac{Q}{h^3}\right) \tag{2.29}$$

which describes the pressure gradient along the length of the system shown in Figure 2-1.

2.4 Pressure Analysis

It is useful to non-dimensionalize Equation (2.29) because the individual terms of the equation can be analyzed. Let

$$\begin{gathered} p = \hat{p}\, p_b \quad , \quad x = \hat{x}\, L_3 \quad , \quad h = \hat{h}\, h_0 \quad , \quad \delta = \hat{\delta} h_0 \quad , \quad w = \hat{w} L_3 \quad , \quad L_1 = \hat{L}_1 L_3 \quad , \\ L_2 = \hat{L}_2 L_3 \quad , \quad Q = \hat{Q}\frac{p_b h_0^{\,3}}{12\mu\, L_3} \quad , \quad U = \hat{U}\frac{p_b h_0^{\,2}}{6\mu\, L_3} \quad , \quad F = \hat{F} p_b L_3 \quad , \quad T = \hat{T} p_b L_3^{\,2} \end{gathered} \tag{2.30}$$

where p_b indicates the pressure at $x = L_3$, h_0 is the fluid film thickness, F is the total force per unit width and T is the total torque per unit width acting on the system. Here the terms with the carets are dimensionless. Substituting the above values in Equation (2.29), the non-dimensional form is given by

$$\frac{\partial \hat{p}}{\partial \hat{x}} = \left(\frac{\hat{U}}{\hat{h}^2} - \frac{\hat{Q}}{\hat{h}^3}\right) \tag{2.31}$$

Equation (2.31) is solved to determine the pressures in segments 1, 2 and 3. Note: This equation can be re-dimensionalized by substituting Equation (2.30) back into (2.31). Considering the film thickness *h* at each section of the system,

$$h=\begin{cases} h_1 = h_0, & 0 < x < L_1 \\ h_2 = h_0 + \delta, & L_1 < x < L_2 \\ h_3 = h_0, & L_2 < x < L_3 \end{cases} \tag{2.32}$$

substituting Equations $h = \hat{h}\ h_0$, $\delta = \hat{\delta} h_0$ from (2.30), Equation (2.32) reduces to

$$\hat{h}=\begin{cases} \hat{h}_1 = 1, & 0 < \hat{x} < \hat{L}_1 \\ \hat{h}_2 = 1 + \hat{\delta}, & \hat{L}_1 < \hat{x} < \hat{L}_2 \\ \hat{h}_3 = 1, & \hat{L}_2 < \hat{x} < 1 \end{cases} \tag{2.33}$$

Thus Equation (2.31) for the pressure differential along segments 1, 2 and 3 are given by

$$\frac{\partial \hat{p}_1}{\partial \hat{x}} = \left(\hat{U} - \hat{Q}\right) \tag{2.34}$$

$$\frac{\partial \hat{p}_2}{\partial \hat{x}} = \left(\frac{\hat{U}}{(1+\hat{\delta})^2} - \frac{\hat{Q}}{(1+\hat{\delta})^3}\right) \tag{2.35}$$

$$\frac{\partial \hat{p}_3}{\partial \hat{x}} = \left(\hat{U} - \hat{Q}\right) \tag{2.36}$$

Integrating Equations (2.34) through (2.36) to determine the pressures at segment 1, 2 and 3

$$\hat{p}_1 = \int \frac{\partial \hat{p}_1}{\partial \hat{x}} + C_1 = (\hat{U} - \hat{Q})\hat{x} + C_1 \tag{2.37}$$

$$\hat{p}_2 = \int \frac{\partial \hat{p}_2}{\partial \hat{x}} + C_2 = \frac{(\hat{U} - \hat{Q} + \hat{U}\hat{\delta})x}{(1+\hat{\delta})^3} + C_2 \tag{2.38}$$

$$\hat{p}_3 = \int \frac{\partial \hat{p}_3}{\partial \hat{x}} + C_3 = (\hat{U} - \hat{Q})\hat{x} + C_3 \tag{2.39}$$

Integration constants C_1, C_2, C_3 and volumetric flow rate $\hat{Q}$ can be determined by considering the following boundary conditions.

$$\hat{p}_1(x=0) \;=\; 0 \tag{2.40}$$

$$\hat{p}_1(x=\hat{L}_1) \;=\; \hat{p}_2(x=\hat{L}_1) \tag{2.41}$$

$$\hat{p}_2(x=\hat{L}_1+\hat{w}) \;=\; \hat{p}_3(x=\hat{L}_1+\hat{w}) \tag{2.42}$$

$$\hat{p}_3(x=1) \;=\; 1 \tag{2.43}$$

Solving Equations (2.37) through (2.39) for C_1, C_2, C_3 and $\hat{Q}$ yields

$$C_1 \;=\; 0 \tag{2.44}$$

$$C_2 \;=\; \frac{\hat{L}_1\hat{\delta}(R-\hat{U})}{(1+\hat{\delta})^3-\hat{w}\hat{\delta}\hat{R}} \tag{2.45}$$

$$C_3 \;=\; \frac{\hat{w}\hat{\delta}(R-\hat{U})}{-(1+\hat{\delta})^3+\hat{w}\hat{\delta}R} \tag{2.46}$$

$$\hat{Q}=-\frac{(1+\hat{\delta})\left[(1+\hat{\delta})^2(1-\hat{U})-\hat{w}\hat{\delta}(2+\hat{\delta})\right]}{(1+\hat{\delta})^3-\hat{w}\hat{\delta}R} \tag{2.47}$$

where

$$R=(3+3\hat{\delta}+\hat{\delta}^2) \tag{2.48}$$

Substituting Equations (2.44) through (2.47) back into Equations (2.37) through (2.39), the resulting expression for pressures in segments 1, 2 and 3 is given by

$$\hat{p}_1=\hat{x}\left[\hat{U}-\frac{(1+\hat{\delta})[(1-\hat{U})(1+\hat{\delta})^2-\hat{w}\hat{\delta}(2+\hat{\delta})]}{(1+\hat{\delta})^3-R\hat{w}\hat{\delta}}\right] \tag{2.49}$$

$$\hat{p}_2=\frac{\hat{L}_1(R-\hat{U})\hat{\delta}}{(1+\hat{\delta})^3-R\hat{w}\hat{\delta}}+\hat{x}\frac{\left[\hat{U}(1+\hat{\delta})-\frac{(1+\hat{\delta})[(1-\hat{U})(1+\hat{\delta})^2-\hat{w}\hat{\delta}(2+\hat{\delta})]}{(1+\hat{\delta})^3-R\hat{w}\hat{\delta}}\right]}{(1+\hat{\delta})^3} \tag{2.50}$$

$$\hat{p}_3 = \frac{(R-\hat{U})\hat{w}\hat{\delta}}{R\hat{w}\hat{\delta}-(1+\hat{\delta})^3} + \hat{x}\left[\hat{U} - \frac{(1+\hat{\delta})[(1-\hat{U})(1+\hat{\delta})^2 - \hat{w}\hat{\delta}(2+\hat{\delta})]}{(1+\hat{\delta})^3 - R\hat{w}\hat{\delta}}\right] \quad (2.51)$$

Variation of pressure along the length of the flat plate is now plotted for segments 1, 2 and 3. Considering nominal values of $\hat{\delta} = 40$, $\hat{U} = 10$, $\hat{L}_1 = 0.25$, $\hat{L}_2 = 0.75$ and $\hat{w} = 0.5$, the plot is as shown below.

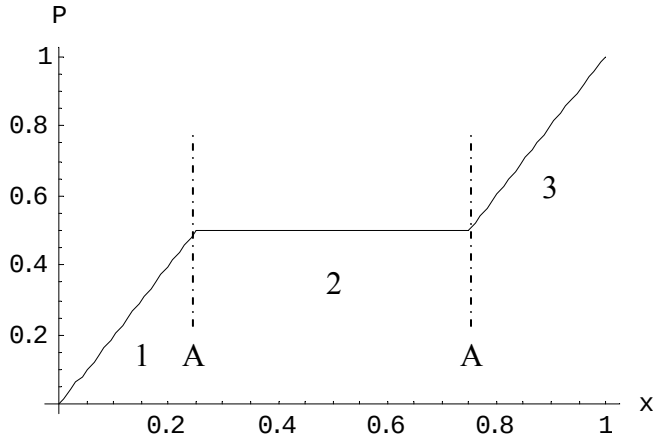

Figure 2-2. Pressure variation of the straight flat plate at segments 1, 2 and 3.

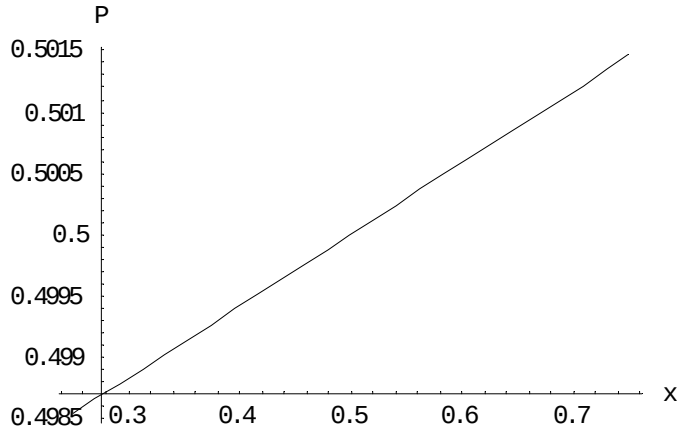

Figure 2-3. Pressure variation between section A-A.

The variation of pressure along the width of the groove (Section A-A) is shown enlarged in Figure 2-3 for clarity and shows that pressure is not constant but varies linearly along the groove.

2.5 Force Analysis

Now that the pressure analysis is done, the force that is accompanied by the pressure differential along the length of the flat plate system is analyzed. This force acts between the flat plates keeping them parallel to each other. The total force F acting on the system is the sum of the individual forces in sections 1, 2 and 3 and is as shown below.

$$\hat{F} = \int_0^{\hat{L}_1} \hat{p}_1 d\hat{x} + \int_{\hat{L}_1}^{\hat{L}_1+\hat{w}} \hat{p}_2 d\hat{x} + \int_{\hat{L}_1+\hat{w}}^{1} \hat{p}_3 d\hat{x} \tag{2.52}$$

Substituting Equations (2.49) through (2.51) in Equation (2.52) yields

$$\begin{aligned}\hat{F} = & \int_0^{\hat{L}_1} \left[(\hat{U} - \hat{Q})\hat{x} + C_1 \right] d\hat{x} + \int_{\hat{L}_1}^{\hat{L}_1+\hat{w}} \left[\frac{(\hat{U} - \hat{Q} + \hat{U}\hat{\delta})\hat{x}}{(1+\hat{\delta})^3} + C_2 \right] d\hat{x} + \\ & \int_{\hat{L}_1+\hat{w}}^{1} \left[(\hat{U} - \hat{Q})\hat{x} + C_3 \right] d\hat{x}\end{aligned} \tag{2.53}$$

and solving them, the total force acting on the system is given by

$$\hat{F} = \frac{\hat{U}\hat{w}\hat{\delta} + (1+\hat{\delta})^3 + \hat{w}(2\hat{L}_1 + \hat{w})\hat{\delta}R - \hat{w}\hat{\delta}\left[\hat{U}(2\hat{L}_1 + \hat{w}) + 2R \right]}{2\left[(1+\hat{\delta})^3 - \hat{w}\hat{\delta}R \right]} \tag{2.54}$$

Equation (2.54) shows that the total force $\hat{F}$ depends on Length $\hat{L}_1$, width $\hat{w}$, groove depth $\hat{\delta}$ and sliding velocity $\hat{U}$ of the flat plate system.

2.6 Torque Analysis

The force that tends to cause rotation is called torque and is determined by multiplying the applied force by the distance from the pivot point to the point where the force is applied. Torque acting in this flat plate system tends to keep the flat plates unparallel to each other. The total torque $\hat{T}$ acting on the system is

$$\hat{T} = \int_0^{\hat{L}_1} \hat{p}_1 \, \hat{x} d\hat{x} + \int_{\hat{L}_1}^{\hat{L}_1+\hat{w}} \hat{p}_2 \, \hat{x} d\hat{x} + \int_{\hat{L}_1+\hat{w}}^{1} \hat{p}_2 \, \hat{x} d\hat{x} \tag{2.55}$$

Substituting the values of pressures $\hat{p}_1$, $\hat{p}_2$ and $\hat{p}_3$ from Equations (2.49) through (2.51) in Equation (2.55),

$$\begin{aligned} \hat{T} = & \int_0^{\hat{L}_1} \left[(\hat{U} - \hat{Q})\hat{x} + C_1 \right] \hat{x} d\hat{x} + \int_{\hat{L}_1}^{\hat{L}_1+\hat{w}} \left[\frac{(\hat{U} - \hat{Q} + \hat{U}\hat{\delta})\hat{x}}{(1+\hat{\delta})^3} + C_2 \right] \hat{x} d\hat{x} + \\ & \int_{\hat{L}_1+\hat{w}}^{1} \left[(\hat{U} - \hat{Q})\hat{x} + C_3 \right] \hat{x} d\hat{x} \end{aligned} \tag{2.56}$$

Solving the above equation, the expression for the total torque is given by

$$\hat{T} = \frac{\hat{U}\hat{w}\hat{\delta}\left[1 - (3\hat{L}_1^{\,2} + 3\hat{L}_1\hat{w} + \hat{w}^2)\right] + 2(1+\hat{\delta})^3 + \hat{w}\hat{\delta}R\left[(3\hat{L}_1^{\,2} + 3\hat{L}_1\hat{w} + \hat{w}^2) - 3\right]}{6\left[(1+\hat{\delta})^3 - \hat{w}\hat{\delta}R\right]} \tag{2.57}$$

Equations (2.54) and (2.57) shows that the parameters on which the total force & torque depend are length $\hat{L}_1$, width of the groove $\hat{w}$, depth of the groove $\hat{\delta}$ and sliding velocity $\hat{U}$. By varying these parameters it is possible to determine the importance of each parameter on the lubrication effects and this will help single out the most significant entity. This process of singling out parameters is discussed in the next section.

2.7 Sensitivity

Sensitivity is the process of analyzing the design parameters having the largest impact on a system and singling them out. Sensitivity coefficients of flow rate, force and torque for the flat plate system are now analyzed in this section.

Consider Equation (2.47), which is the flow rate in the flat plate system and is shown here again.

$$\hat{Q} = -\frac{(1+\hat{\delta})\left((1+\hat{\delta})^2(1-\hat{U}) - \hat{w}\hat{\delta}(2+\hat{\delta})\right)}{(1+\hat{\delta})^3 - \hat{w}\hat{\delta}R} \tag{2.58}$$

The parameters on which the flow rate depends are groove width $\hat{w}$ and groove depth $\hat{\delta}$. Notice that Equation (2.58) does not contain length $\hat{L}_1$, which indicates that the flow rate is independent of the effects of length $\hat{L}_1$. The Taylor series of expansion for the flow rate is given by:

$$\hat{Q} \;=\; \hat{Q}_0 + \left(\frac{\partial \hat{Q}}{\partial \hat{w}}\bigg|_0\right)(\hat{w}-\hat{w}_0) + \left(\frac{\partial \hat{Q}}{\partial \hat{\delta}}\bigg|_0\right)(\hat{\delta}-\hat{\delta}_0) \tag{2.59}$$

where $_0$ denotes the nominal condition. The sensitivity coefficients of the flow rate with respect to parameters $\hat{w}$ and $\hat{\delta}$ are calculated and are given by:

$$\frac{\partial \hat{Q}}{\partial \hat{w}} = -\frac{\hat{\delta}(1+\hat{\delta})^3(R-\hat{U})}{\left[(\hat{w}-1)\hat{\delta}R - 1\right]^2} \tag{2.60}$$

$$\frac{\partial \hat{Q}}{\partial \hat{\delta}} = \frac{\hat{w}\left[-3(1+\hat{\delta})^2 + \hat{U}\left(1+(\hat{w}-1)\hat{\delta}^2(3+2\hat{\delta})\right)\right]}{\left[(\hat{w}-1)\hat{\delta}R - 1\right]^2} \tag{2.61}$$

Similarly the sensitivity coefficients of force and torque are analyzed. Equations (2.54) and (2.57) showed that the important parameters on which the sensitivity coefficients

depend are length $\hat{L}_1$, depth of groove $\hat{\delta}$ and width of groove $\hat{w}$. The Taylor series of expansion for the total force for these parameters is given by

$$\hat{F} = \hat{F}_0 + \left(\frac{\partial \hat{F}}{\partial \hat{L}_1}\bigg|_0 \right)(\hat{L}_1 - \hat{L}_{1_0}) + \left(\frac{\partial \hat{F}}{\partial \hat{w}}\bigg|_0 \right)(\hat{w} - \hat{w}_0) + \left(\frac{\partial \hat{F}}{\partial \hat{\delta}}\bigg|_0 \right)(\hat{\delta} - \hat{\delta}_0) \qquad (2.62)$$

The sensitivity coefficients of the force with respect to the parameters $\hat{L}_1$, $\hat{\delta}$ and $\hat{w}$ are calculated and are as shown below.

$$\frac{\partial \hat{F}}{\partial \hat{L}_1} = \frac{\hat{w}\hat{\delta}(R - \hat{U})}{(1+\hat{\delta})^3 - \hat{w}\hat{\delta}R} \qquad (2.63)$$

$$\frac{\partial \hat{F}}{\partial \hat{w}} = \frac{\hat{\delta}(R - \hat{U})\left[(1+\hat{\delta})^3(2\hat{L}_1 + 2\hat{w} - 1) - \hat{w}^2\hat{\delta}R \right]}{2\left[R\hat{\delta}(\hat{w} - 1) - 1 \right]^2} \qquad (2.64)$$

$$\frac{\partial \hat{F}}{\partial \hat{\delta}} = -\frac{\hat{w}(\hat{w} - 1 + 2\hat{L}_1)\left[-3(1+\hat{\delta})^2 + \hat{U}\left(1 + (\hat{w}-1)\hat{\delta}^2(3+2\hat{\delta})\right) \right]}{2\left[\hat{\delta}R(\hat{w} - 1) - 1 \right]^2} \qquad (2.65)$$

Similarly the Taylor series of expansion for the torque is given by

$$\hat{T} = \hat{T}_0 + \left(\frac{\partial \hat{T}}{\partial \hat{L}_1}\bigg|_0 \right)(\hat{L}_1 - \hat{L}_{1_0}) + \left(\frac{\partial \hat{T}}{\partial \hat{w}}\bigg|_0 \right)(\hat{w} - \hat{w}_0) + \left(\frac{\partial \hat{T}}{\partial \hat{\delta}}\bigg|_0 \right)(\hat{\delta} - \hat{\delta}_0) \qquad (2.66)$$

where,

$$\frac{\partial \hat{T}}{\partial \hat{L}_1} = -\frac{\hat{w}\hat{\delta}(R - \hat{U})(2\hat{L}_1 + \hat{w})}{-2 + 2(\hat{w} - 1)\hat{\delta}R} \qquad (2.67)$$

$$\frac{\partial \hat{T}}{\partial \hat{w}} = \frac{\hat{\delta}(R - \hat{U})\left[(1+\hat{\delta})^3(3\hat{L}_1^{\,2} + 3\hat{w}^2 - 1) - 2\hat{w}^3\hat{\delta}R - 3\hat{L}_1\hat{w}\left((\hat{w} - 2)\hat{\delta}R - 2 \right) \right]}{6\left[\hat{\delta}R(\hat{w} - 1) - 1 \right]^2} \qquad (2.68)$$

$$\frac{\partial \hat{T}}{\partial \hat{\delta}} = -\frac{\hat{w}\left(3\hat{L}_1(\hat{L}_1 + \hat{w}) + \hat{w}^2 - 1 \right)\left[-3(1+\hat{\delta})^2 + \hat{U}\left(1 + (\hat{w}-1)\hat{\delta}^2(3+2\hat{\delta})\right) \right]}{6\left[\hat{\delta}R(\hat{w} - 1) - 1 \right]^2} \qquad (2.69)$$

The results of the sensitivity coefficients of flow rate $\hat{Q}$, force $\hat{F}$ and torque $\hat{T}$ will be discussed in the next chapter. These equations indicate the importance of each parameter in the analysis of the lubrication groove and also help determine the design aspects that need to be implemented to improve the lubrication in the flat plate system.

2.8 Dimensional Results

The equations in the previous sections were written in the non-dimensional form and now those equations will be converted back to its dimensional form. Substituting Equations (2.10) and (2.30) into Equations (2.47), (2.54) and (2.57), the dimensional form of the flow rate Q, total force F and total torque T are

$$Q = -\frac{{h_0}^3}{12\mu}\left[\frac{(h_0+\delta)\left(({h_0}^2-6\mu U)(h_0+\delta)^2 - w\delta(\delta+2h_0)\right)}{(h_0+\delta)^3 - w\delta(\delta^2+3\delta h_0+3{h_0}^2)}\right] \tag{2.70}$$

$$F = \frac{6Uw\delta\mu + (\delta+h_0)^3 + w\delta(\delta^2+3\delta h_0+3{h_0}^2)(w+2L_1)}{2\left[(h_0+\delta)^3 - w\delta(\delta^2+3\delta h_0+3{h_0}^2)\right]} - \frac{2w\delta\left[\delta^2+3U\mu(w+2L_1)+3h_0(\delta+h_0)\right]}{2\left[(h_0+\delta)^3 - w\delta(\delta^2+3\delta h_0+3{h_0}^2)\right]} \tag{2.71}$$

$$T = \frac{w\delta(3{h_0}^2+\delta^2+3\delta)\left[3L_1(w+L_1)+w^2-3\right]}{6\left[(h_0+\delta)^3 - w\delta(\delta^2+3\delta h_0+3{h_0}^2\right]} + \frac{2\left[(\delta+h_0)^3+3Uw\mu\delta\left(1-w^2-3L_1(w+L_1)\right)\right]}{6\left[(h_0+\delta)^3 - w\delta(\delta^2+3\delta h_0+3{h_0}^2\right]} \tag{2.72}$$

The dimensional form of the flow coefficients $\frac{\partial Q}{\partial w}$ and $\frac{\partial Q}{\partial \delta}$ are obtained by substituting Equations (2.10) and (2.30) into Equations (2.60) and (2.61).

$$\frac{\partial Q}{\partial w} = \frac{\delta(\delta+h_0)^3\left[\delta^2-6\mu U+3h_0(\delta+h_0)\right]}{12\mu\left[(w-1)\delta\left(\delta^2+3\delta h_0+3{h_0}^2\right)-{h_0}^3\right]} \tag{2.73}$$

$$\frac{\partial Q}{\partial \delta} = \frac{w\left[6\mu U\left(h_0{}^3 + (w-1)\delta^2(2\delta + 3h_0)\right) - 3(h_0+\delta)^2 h_0{}^3\right]}{12\mu\left[(w-1)\delta(\delta^2 + 3\delta h_0 + 3h_0{}^2) - h_0{}^3\right]} \tag{2.74}$$

Sensitivity of the force coefficients are obtained by substituting Equations (2.10) and (2.30) into Equations (2.63) through (2.65) and are as shown below.

$$\frac{\partial F}{\partial L_1} = \frac{w\delta\left[\delta^2 - 6\mu U + 3h_0(\delta + h_0)\right]}{\delta(w-1)(\delta^2 + 3\delta h_0 + 3h_0{}^2) - h_0{}^3} \tag{2.75}$$

$$\frac{\partial F}{\partial w} = \frac{\left[\begin{array}{l}\left(3h_0{}^2 + (\delta^2 - 6\mu U) + 3\delta h_0\right) \text{ x} \\ \left((\delta + h_0)^3(2w + 2L_1 - 1) - w^2\delta[\delta^2 + 3h_0(\delta + h_0)]\right)\end{array}\right]}{2\left[\delta + \left(\delta^2 + 3h_0(\delta + h_0)\right) - h_0{}^3\right]^2} \tag{2.76}$$

$$\frac{\partial F}{\partial \delta} = -\frac{\left[w(2L_1 + w - 1)\left(-3(h_0+\delta)^2 h_0{}^3 + 6\mu U[(w-1)\delta^2(3h_0 + 2\delta) + h_0{}^3]\right)\right]}{2\left[(w-1)\delta^2(3h_0 + 2\delta) + h_0{}^3\right]^2} \tag{2.77}$$

Similarly the torque coefficients are obtained by putting in Equations (2.10) and (2.30) into torque Equations (2.67) through (2.69).

$$\frac{\partial T}{\partial L_1} = \frac{w\delta(w + 2L_1)\left[\delta^2 - 6\mu U + 3h_0(\delta + h_0)\right]}{2\left[(1-w)\delta\left(\delta^2 + 3\delta h_0 + 3h_0{}^2\right) + h_0{}^3\right]} \tag{2.78}$$

$$\frac{\partial T}{\partial w} = \frac{\left[\begin{array}{l}\delta\left(3h_0{}^2 + (\delta^2 - 6\mu U) + 3\delta h_0\right)\{-2w^3\delta\left(\delta^2 + 3h_0(\delta + h_0)\right) + \\ (h_0 + \delta)\left(3(w^2 + L_1{}^2) - 1\right) - 3L_1 w\left((w-2)\delta(\delta^2 + 3\delta h_0 + 3h_0{}^2) - 2h_0{}^3\right)\}\end{array}\right]}{6\left[(w-1)\delta(\delta^2 + 3\delta h_0 + 3h_0{}^2) - h_0{}^3\right]^2} \tag{2.79}$$

$$\frac{\partial T}{\partial \delta} = \frac{\left[\begin{array}{l}-w\left(w^2 - 1 + 3L_1(w + L_1)\right) \text{ x} \\ \left[-3(h_0+\delta)^2 h_0{}^3 + 6\mu U\left(h_0{}^3 + (w-1)\delta^2(3h_0 + 2\delta)\right)\right]\end{array}\right]}{6\left[(w-1)\delta(\delta^2 + 3\delta h_0 + 3h_0{}^2) - h_0{}^3\right]^2} \tag{2.80}$$

Equations (2.70) through (2.80) are the complete lubrication analysis results of flow rate, force and torque in its dimensional form. The reason for conversion from non-dimensional to dimensional form is that results are best explained to an Engineer for calculations in dimensional form and also that they help in quantifying the magnitude of the results.

2.9 Conclusion

In the previous subsections, Reynolds equation for low Reynolds number flow was derived from the Navier Stokes equation. This equation was solved for the pressure differential and then non-dimensionalized by applying the expressions in Equation (2.30). The reasoning behind this technique was to produce a dimensionless equation that will contain constants to determine the significance of the individual transient terms. Pressure, force and torque acting on a straight flat plate system were analyzed and expressions for each of them were derived. Finally sensitivity analysis of flow rate, force and torque to determine the importance of the system parameters was carried out.

CHAPTER 3. RESULTS AND DISCUSSION

3.1 Introduction

The previous chapter discussed the equations of the flat plate system for flow rate, total force and torque and also their respective sensitivities. In this chapter, two cases of groove length, for analysis of the flat plate system is considered. The results of the flow rate, flow force and torque sensitivity acting on them will be tabulated and also plotted. These results will indicate the importance of the parameters that affect the lubrication and the significance of each of them in the lubrication improvement of the system.

3.2 Geometry Considerations

The two cases of the groove for the flat plate system analyzed in this chapter are shown in the following figures:

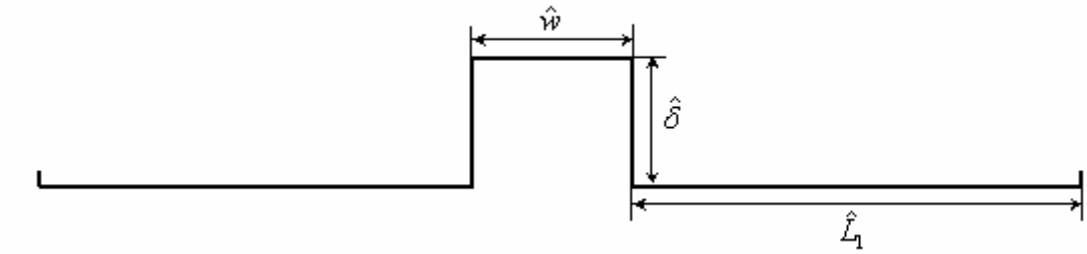

Figure 3-1. Groove width is small & deep depth.

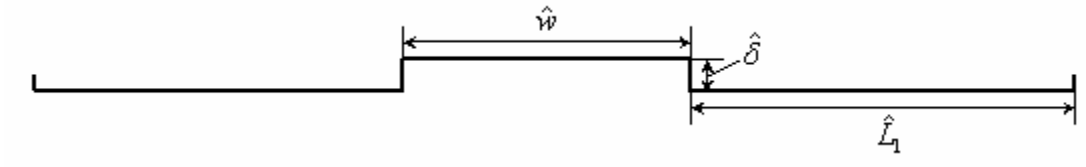

Figure 3-2. Groove width is long & shallow depth.

Where $\hat{w}$ is the groove width, $\hat{\delta}$ is the groove depth and $\hat{L}_1$ is the length till the start of the groove as shown in Figures 3-1 and 3-2.

As the groove case in Figure 3-1 is the type most commonly used, to consider the lubrication effects of other possible cases, a groove with long width and shallow depth is considered as shown in Figure 3-2. These two cases are analyzed at sliding velocities of $\hat{U} = -10, 0$ and 10. Sliding velocities given by $\hat{U} = -10, 0$ and 10 indicate that the flat plate is moving in the positive *x* direction, standing still and in the negative *x* direction respectively. The reference source of equations to plot the values of the sensitivities are given by Equations (2.60), (2.61), (2.63) through (2.65) and (2.67) through (2.69) from Chapter 2.

In this chapter, the results are tabulated for the sensitivities of flow rate, force and torque considering the nominal conditions. The nominal conditions for the flat plate system considered are given by:

For groove with small width as shown in Figure 3-1,

$$\hat{\delta} = 40;\ \hat{w} = 0.03;\ \hat{L}_1 = 0.485 \tag{3.1}$$

For groove with long width as shown in Figure 3-2,

$$\hat{\delta} = 1;\ \hat{w} = 0.25;\ \hat{L}_1 = 0.375 \tag{3.2}$$

The discussion of flow rate, force and torque sensitivity results are done in the subsequent sections. Note: The difference between $\hat{\delta}$ for small groove width and long groove width is large as seen in Equations (3.1) and (3.2).

3.3 Volumetric Flow Rate Sensitivity

The small gap between the moving flat plate and housing holds a certain amount of lubricating medium and this section analyzes the flow rate of this lubricant and the various factors of the flat plate system that influences this flow rate.

3.3.1 Flow Results

Consider the flow rate Equation (2.58) from Chapter 2 given by:

$$\hat{Q} = -\frac{(1+\hat{\delta})\left((1+\hat{\delta})^2(1-\hat{U}) - \hat{w}\hat{\delta}(2+\hat{\delta})\right)}{(1+\hat{\delta})^3 - \hat{w}\hat{\delta}R} \tag{3.3}$$

where

$$R = (3 + 3\hat{\delta} + \hat{\delta}^2) \tag{3.4}$$

Equation (3.3) clearly indicates that the factors of influence for the flow rate are the depth of the groove $\hat{\delta}$ and the width of the groove $\hat{w}$. Considering the sensitivity coefficients of the flow rate with respect to these two parameters, the resulting Equations (2.60) and (2.61) from Chapter 2 are given by:

$$\frac{\partial \hat{Q}}{\partial \hat{w}} = -\frac{\hat{\delta}(1+\hat{\delta})^3(R-\hat{U})}{\left[(\hat{w}-1)\hat{\delta}R - 1\right]^2} \tag{3.5}$$

$$\frac{\partial \hat{Q}}{\partial \hat{\delta}} = \frac{\hat{w}\left[-3(1+\hat{\delta})^2 + \hat{U}\left(1 + (\hat{w}-1)\hat{\delta}^2(3+2\hat{\delta})\right)\right]}{\left[(\hat{w}-1)\hat{\delta}R - 1\right]^2} \tag{3.6}$$

Equations (3.5) and (3.6) show that of the flow rate sensitivity is independent of the length $\hat{L}_1$. This is a very important inference from the flow sensitivity point of view,

which indicates that one would not need to bother about the placement of the groove along x direction if one is trying to alter the flow rate. The above equations also show that sliding velocity $\hat{U}$ holds some influence in the flow sensitivity analysis, the effects of which will be further discussed in the subsequent sections.

Now the results for the sensitivity coefficients for the flow rate with respect to groove width and groove depth are tabulated and shown in Tables 3-1 through 3-3. The nominal conditions considered for each groove width case to get these results are given by Equations (3.1) and (3.2).

	SHORT WIDTH $\hat{U}=10$			LONG WIDTH $\hat{U}=10$		
	$\hat{w}=0.027$	$\hat{w}=0.03$	$\hat{w}=0.033$	$\hat{w}=0.225$	$\hat{w}=0.25$	$\hat{w}=0.275$
$\frac{\partial \hat{Q}}{\partial \hat{w}}$	-1.05	-1.057	-1.063	0.581	0.614	0.65
	$\hat{\delta}=36$	$\hat{\delta}=40$	$\hat{\delta}=44$	$\hat{\delta}=0.9$	$\hat{\delta}=1$	$\hat{\delta}=1.1$
$\frac{\partial \hat{Q}}{\partial \hat{\delta}}$	-1.18E-05	-8.68E-06	-6.59E-06	-0.258	-0.253	-0.243

Table 3-1. Sensitivity coefficients of flow rate for nominal conditions $\hat{w}$ and $\hat{\delta}$ at sliding velocity $\hat{U}=10$. Nominal conditions given by Equations (3.1) and (3.2).

	SHORT WIDTH $\hat{U}=0$			LONG WIDTH $\hat{U}=0$		
	$\hat{w}=0.027$	$\hat{w}=0.03$	$\hat{w}=0.033$	$\hat{w}=0.225$	$\hat{w}=0.25$	$\hat{w}=0.275$
$\frac{\partial \hat{Q}}{\partial \hat{w}}$	-1.056	-1.063	-1.069	-1.357	-1.434	-1.517
	$\hat{\delta}=36$	$\hat{\delta}=40$	$\hat{\delta}=44$	$\hat{\delta}=0.9$	$\hat{\delta}=1$	$\hat{\delta}=1.1$
$\frac{\partial \hat{Q}}{\partial \hat{\delta}}$	-4.57E-08	-3.03E-08	-2.09E-08	-0.093	-0.077	-0.064

Table 3-2. Sensitivity coefficients of flow rate for nominal conditions $\hat{w}$ and $\hat{\delta}$ at sliding velocity $\hat{U}=0$. Nominal conditions given by Equations (3.1) and (3.2).

	SHORT WIDTH $\hat{U}=-10$			LONG WIDTH $\hat{U}=-10$		
	$\hat{w}=0.027$	$\hat{w}=0.03$	$\hat{w}=0.033$	$\hat{w}=0.225$	$\hat{w}=0.25$	$\hat{w}=0.275$
$\frac{\partial \hat{Q}}{\partial \hat{w}}$	-1.062	-1.069	-1.076	-3.295	-3.482	-3.685
	$\hat{\delta}=36$	$\hat{\delta}=40$	$\hat{\delta}=44$	$\hat{\delta}=0.9$	$\hat{\delta}=1$	$\hat{\delta}=1.1$
$\frac{\partial \hat{Q}}{\partial \hat{\delta}}$	1.04E-05	7.73E-06	5.87E-06	0.072	0.099	0.116

Table 3-3. Sensitivity coefficients of flow rate for nominal conditions $\hat{w}$ and $\hat{\delta}$ at sliding velocity $\hat{U}=-10$. Nominal conditions given by Equations (3.1) and (3.2).

Tables 3-1 through 3-3 show that the values of flow rate sensitivity with respect to groove width $\hat{w}$ are higher in all the three sliding velocity cases and can be seen that its magnitude is greater compared to flow sensitivity for groove depth. This clearly shows that for effective control for flow rate sensitivity, changes in groove width have a more significant effect and that groove depth could be least considered in flow rate analysis for the flat plate system considered. Also an interesting aspect to notice in Table 3-1 is that flow sensitivity $\frac{\partial \hat{Q}}{\partial \hat{w}}$ changes its sign when the groove width is changed from short to long for the same sliding velocity. The explanation is given in Equation (3.5), where the quantity that influences the change of flow sensitivity sign is $R-\hat{U}$, as the rest of the terms in the equation are positive. Thus for a positive sliding velocity $\hat{U}$, when the groove width changes from short to long, groove depth $\hat{\delta}$ changes from a higher value to a lower value i.e. from 40 to 1, thus resulting in a change of flow sensitivity sign.

The three values for each sensitivity as shown in Tables 3-1 through 3-6 for both short and long width cases is because the sensitivity parameter has been varied along the nominal values i.e. one value each at $\pm 10\%$ of the nominal value and one value at the

nominal condition. For nominal conditions of the flat plate, length $\hat{L}_1$ is varied by a tenth of the grove width $\hat{w}$, whereas groove depth $\hat{\delta}$ and groove width $\hat{w}$ is varied by ±10% of its nominal value respectively.

Now that the tables have been tabulated, the plots for the flow rate sensitivity for clearer understanding of the above tables are shown below from Figures 3-3 through 3-8. The plots from Figure 3-3 through 3-5 show that sensitivity lines for both $\frac{\partial \hat{Q}}{\partial \hat{\delta}}$ and $\frac{\partial \hat{Q}}{\partial \hat{w}}$ are almost flat which indicate that sensitivities don't change much with parameter variation for short groove width cases.

Sensitivity plots of flow rates for short groove width geometry conditions for different sliding velocities are plotted below from Figure 3-3 through 3-5.

Case 1: Short width, $\hat{U} = 10$

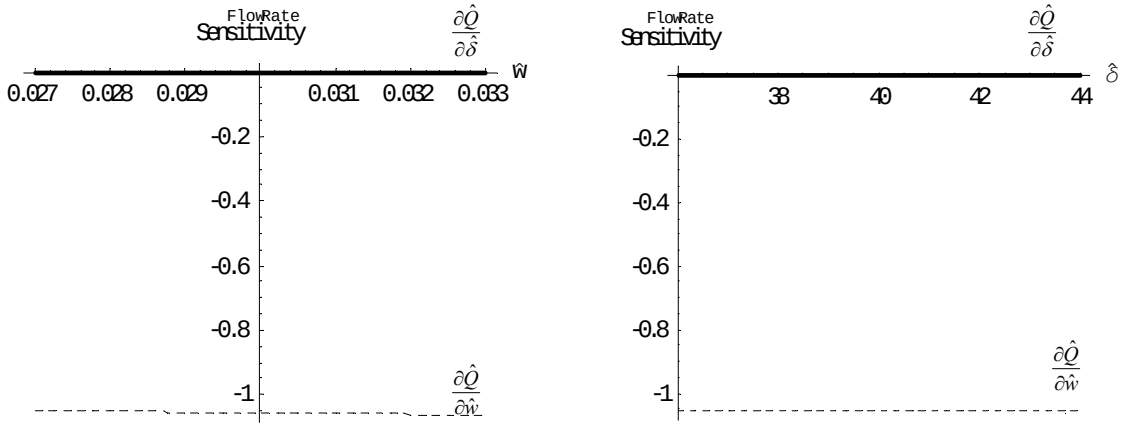

Figure 3-3. Flow rate sensitivity for parameters $\hat{\delta}$ and $\hat{w}$ along width $\hat{w}$ and depth $\hat{\delta}$. Nominal conditions are $\hat{\delta} = 40;\ \hat{w} = 0.03;\ \hat{L}_1 = 0.485$.

Case 2: Short width, $\hat{U} = 0$

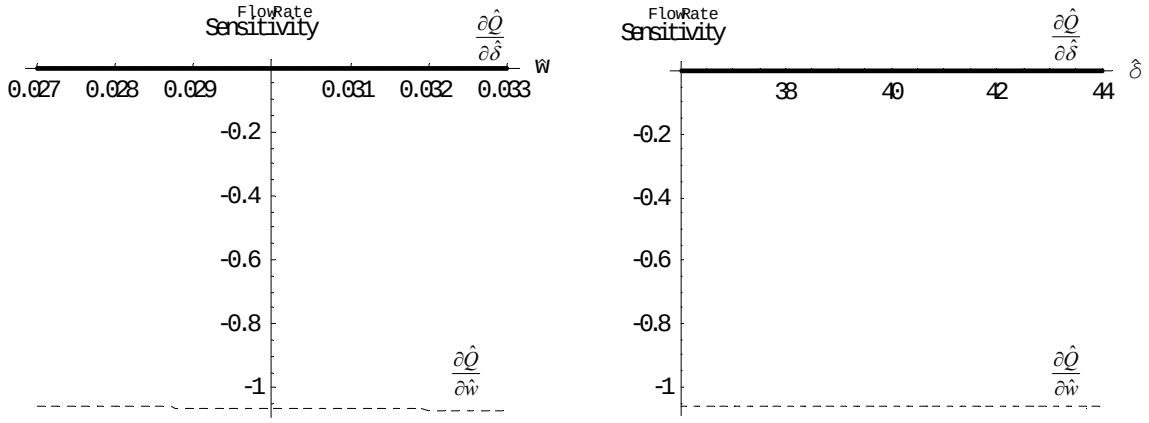

Figure 3-4. Flow rate sensitivity for parameters $\hat{\delta}$ and $\hat{w}$ along width $\hat{w}$ and depth $\hat{\delta}$. Nominal conditions are $\hat{\delta} = 40;\ \hat{w} = 0.03;\ \hat{L}_1 = 0.485$.

Case 3: Short width, $\hat{U} = -10$

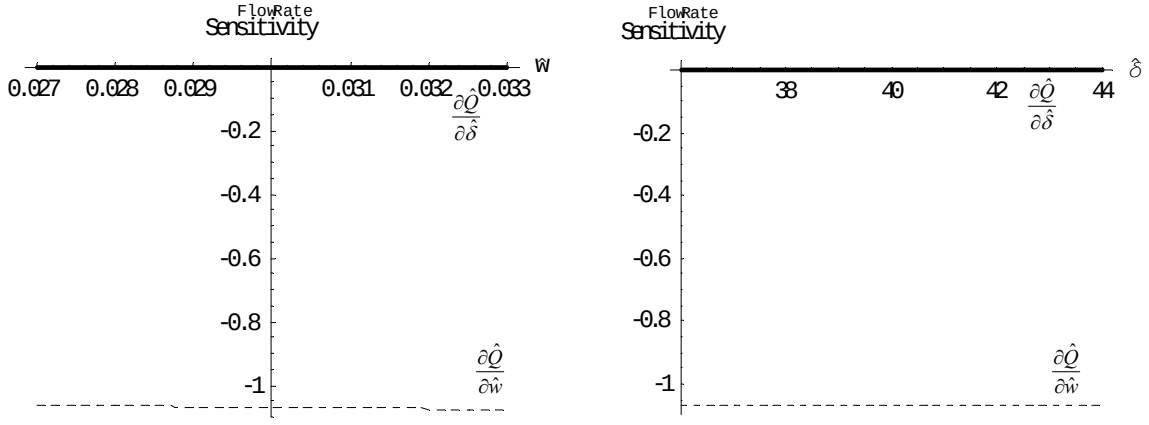

Figure 3-5. Flow rate sensitivity for parameters $\hat{\delta}$ and $\hat{w}$ along width $\hat{w}$ and depth $\hat{\delta}$. Nominal conditions are $\hat{\delta} = 40;\ \hat{w} = 0.03;\ \hat{L}_1 = 0.485$.

Sensitivity plots of flow rates for long groove width geometry conditions for different sliding velocities are plotted below from Figure 3-6 through 3-8.

Case 4: Long width, $\hat{U} = 10$

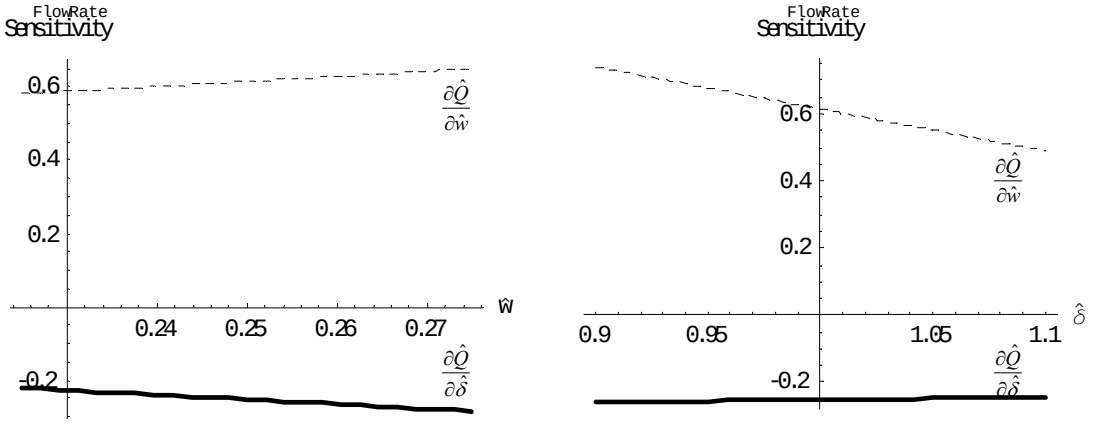

Figure 3-6. Flow rate sensitivity for parameters $\hat{\delta}$ and $\hat{w}$ along width $\hat{w}$ and depth $\hat{\delta}$. Nominal conditions are $\hat{\delta} = 1;\ \hat{w} = 0.25;\ \hat{L}_1 = 0.375$.

Case 5: Long width, $\hat{U} = 0$

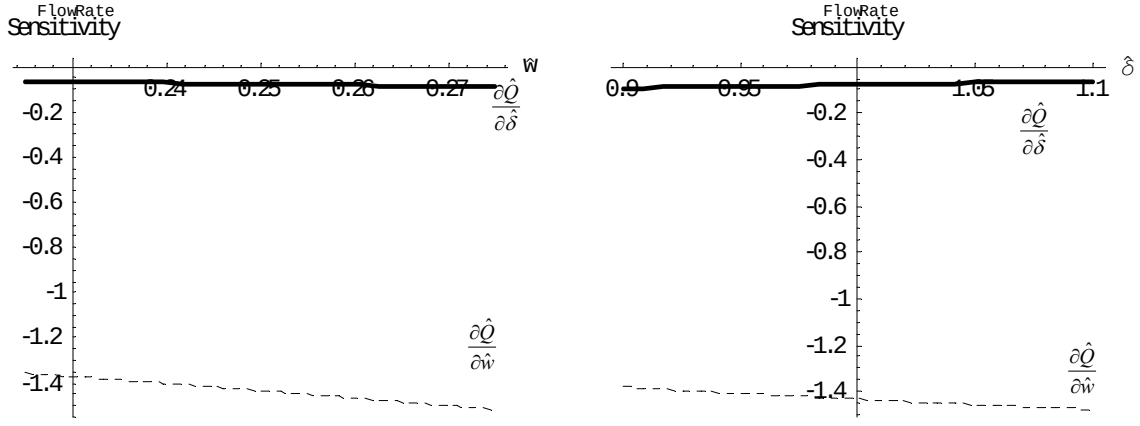

Figure 3-7. Flow rate sensitivity for parameters $\hat{\delta}$ and $\hat{w}$ along width $\hat{w}$ and depth $\hat{\delta}$. Nominal conditions are $\hat{\delta} = 1;\ \hat{w} = 0.25;\ \hat{L}_1 = 0.375$.

Case 6: Long width, $\hat{U} = -10$

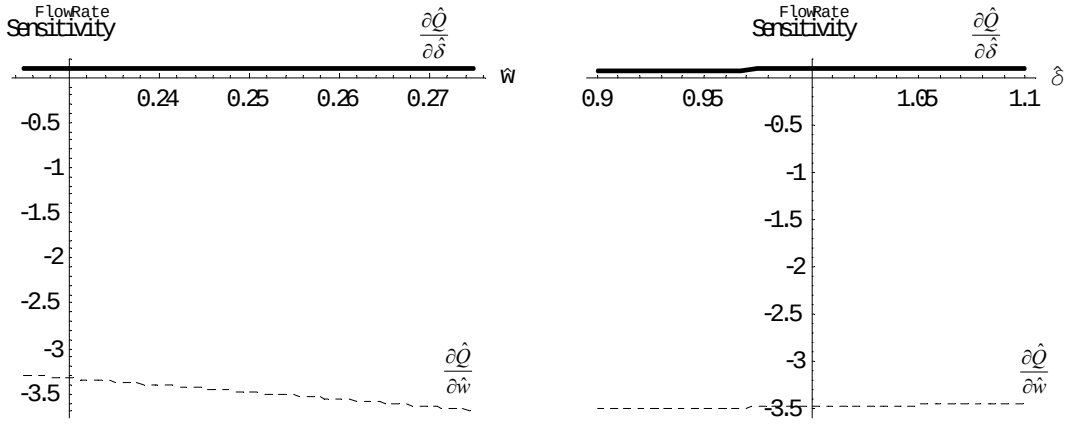

Figure 3-8. Flow rate sensitivity for parameters $\hat{\delta}$ and $\hat{w}$ along width $\hat{w}$ and depth $\hat{\delta}$. Nominal conditions are $\hat{\delta} = 1;\ \hat{w} = 0.25;\ \hat{L}_1 = 0.375$.

Figures 3-6 through 3-8 show that the plotted lines for both flow rate sensitivities with respect to $\hat{w}$ and $\hat{\delta}$ are varying with the nominal conditions which indicate that flow sensitivities change much with parameter variation for long groove width cases.

3.3.2 Discussion for Flow Sensitivity with Respect to Groove Width

Consider the flow rate sensitivity $\frac{\partial \hat{Q}}{\partial \hat{w}}$ given by Equation (3.5). It can be clearly seen from Tables 3-1 through 3-3 that for all groove geometry cases and also for varying sliding velocities, flow sensitivity with respect to $\hat{w}$ has the highest magnitude compared to the flow sensitivity with respect to $\hat{\delta}$. Plots in Figures 3-3 through 3-8 also validate this. This indicates that for effective flow control, the most influential parameter is groove width $\hat{w}$. Any change in this quantity has a significant effect on the flow rate in a flat plate system.

3.3.3 Discussion for Flow Sensitivity with Respect to Groove Depth

The effects of the flow sensitivity $\frac{\partial \hat{Q}}{\partial \hat{\delta}}$ given by Equation (3.6) are discussed now.

The values from Tables 3-1 through 3-3 show that flow sensitivity with respect to groove depth is very small which helps conclude that the effects of groove depth in flow rate sensitivity analysis is very minimal comparative to groove width. Almost all the plots from Figures 3-3 through 3-8 show that the flow sensitivity line follows the zero coordinate axis, which indicates that its magnitude is very low and can thus be neglected in this analysis.

Another aspect to notice is that plots in Figures 3-3 through 3-5 look similar and thus it can be concluded that the sliding velocity $\hat{U}$ is not very influential in flow rate sensitivity for short width deep groove cases. The same could not be said about long width short groove cases as they vary as seen in Figures 3-6 through 3-8.

Thus from Tables 3-1 through 3-3 and Figures 3-3 through 3-8, flow rate sensitivity results showed that for all groove width geometries, groove width $\hat{w}$ is the most influencing parameter to be taken into consideration comparative to groove depth $\hat{\delta}$ and length $\hat{L}_1$.

3.4 Force Sensitivity

Lifting force of the flat plate against its housing aids in better lubrication because of the lubrication gap created. The sensitivity analysis of this force has been done in Chapter 2 and the sensitivity coefficients of force and its dependence on the individual parameters is as shown in the next section.

3.4.1 Force Results

Consider the force Equation (2.54) from Chapter 2 and are shown here again for convenience.

$$\hat{F} = \frac{\hat{U}\hat{w}\hat{\delta} + (1+\hat{\delta})^3 + \hat{w}(2\hat{L}_1 + \hat{w})\hat{\delta}R - \hat{w}\hat{\delta}\left[\hat{U}(2\hat{L}_1 + \hat{w}) + 2R\right]}{2\left[(1+\hat{\delta})^3 - \hat{w}\hat{\delta}R\right]} \tag{3.7}$$

Equation (3.7) show that the lifting force in the flat plate system depends on the parameters $\hat{L}_1$, $\hat{w}$ and $\hat{\delta}$. The sensitivity coefficients with respect to these are given by:

$$\frac{\partial \hat{F}}{\partial \hat{L}_1} = \frac{\hat{w}\hat{\delta}(R - \hat{U})}{(1+\hat{\delta})^3 - \hat{w}\hat{\delta}R} \tag{3.8}$$

$$\frac{\partial \hat{F}}{\partial \hat{w}} = \frac{\hat{\delta}(R - \hat{U})\left[(1+\hat{\delta})^3(2\hat{L}_1 + 2\hat{w} - 1) - \hat{w}^2\hat{\delta}R\right]}{2\left[R\hat{\delta}(\hat{w} - 1) - 1\right]^2} \tag{3.9}$$

$$\frac{\partial \hat{F}}{\partial \hat{\delta}} = -\frac{\hat{w}(\hat{w} - 1 + 2\hat{L}_1)\left[-3(1+\hat{\delta})^2 + \hat{U}\left(1 + (\hat{w} - 1)\hat{\delta}^2(3 + 2\hat{\delta})\right)\right]}{2\left[\hat{\delta}R(\hat{w} - 1) - 1\right]^2} \tag{3.10}$$

where the value of R is given by Equation (3.4).

Equations (3.8) through (3.10) shows that force sensitivity depends on parameters, length $\hat{L}_1$ along with groove depth $\hat{\delta}$ and grove width $\hat{w}$. These equations will help determine the influence of each parameter when the force sensitivity coefficients are varied with the nominal conditions given by Equations (3.1) and (3.2). The results are calculated for the different cases of sliding velocity $\hat{U}$ and groove width geometry and the respective values are tabulated and shown in Tables 3-4 through 3-6 below. Also seen in these tables is that for all cases of sliding velocity, the value for force

sensitivity $\frac{\partial \hat{F}}{\partial \hat{\delta}}$ are not tabulated. The reason for this being that this force sensitivity was so small that the tool Mathematica could not solve for its value.

	SHORT WIDTH $\hat{U}=10$				LONG WIDTH $\hat{U}=10$		
	$\hat{\delta}=36$	$\hat{\delta}=40$	$\hat{\delta}=44$		$\hat{\delta}=0.9$	$\hat{\delta}=1$	$\hat{\delta}=1.1$
$\frac{\partial \hat{F}}{\partial \hat{\delta}}$	6.50E-19	5.30E-19	4.50E-19		-	-	-
	$\hat{L}_1=0.482$	$\hat{L}_1=0.485$	$\hat{L}_1=0.488$		$\hat{L}_1=0.35$	$\hat{L}_1=0.375$	$\hat{L}_1=0.4$
$\frac{\partial \hat{F}}{\partial \hat{L}_1}$	0.031	0.031	0.031		-0.012	-0.012	-0.012
	$\hat{w}=0.027$	$\hat{w}=0.03$	$\hat{w}=0.033$		$\hat{w}=0.225$	$\hat{w}=0.25$	$\hat{w}=0.275$
$\frac{\partial \hat{F}}{\partial \hat{w}}$	0.012	0.016	0.019		-0.045	-0.06	-0.076

Table 3-4. Sensitivity coefficients of force for $\hat{\delta}$, $\hat{L}_1$ and $\hat{w}$ at sliding velocity $\hat{U}=10$. Nominal conditions given by Equations (3.1) and (3.2).

	SHORT WIDTH $\hat{U}=0$				LONG WIDTH $\hat{U}=0$		
	$\hat{\delta}=36$	$\hat{\delta}=40$	$\hat{\delta}=44$		$\hat{\delta}=0.9$	$\hat{\delta}=1$	$\hat{\delta}=1.1$
$\frac{\partial \hat{F}}{\partial \hat{\delta}}$	1.30E-18	1.00E-18	8.70E-19		-	-	-
	$\hat{L}_1=0.482$	$\hat{L}_1=0.485$	$\hat{L}_1=0.488$		$\hat{L}_1=0.35$	$\hat{L}_1=0.375$	$\hat{L}_1=0.4$
$\frac{\partial \hat{F}}{\partial \hat{L}_1}$	0.031	0.031	0.031		0.28	0.28	0.28
	$\hat{w}=0.027$	$\hat{w}=0.03$	$\hat{w}=0.033$		$\hat{w}=0.225$	$\hat{w}=0.25$	$\hat{w}=0.275$
$\frac{\partial \hat{F}}{\partial \hat{w}}$	0.012	0.015	0.019		0.106	0.14	0.177

Table 3-5. Sensitivity coefficients of force for $\hat{\delta}$, $\hat{L}_1$ and $\hat{w}$ at sliding velocity $\hat{U}=0$. Nominal conditions given by Equations (3.1) and (3.2).

	SHORT WIDTH $\hat{U}=-10$				LONG WIDTH $\hat{U}=-10$		
	$\hat{\delta}=36$	$\hat{\delta}=40$	$\hat{\delta}=44$		$\hat{\delta}=0.9$	$\hat{\delta}=1$	$\hat{\delta}=1.1$
$\frac{\partial \hat{F}}{\partial \hat{\delta}}$	6.50E-19	5.30E-19	4.50E-19		-	-	-
	$\hat{L}_1=0.482$	$\hat{L}_1=0.485$	$\hat{L}_1=0.488$		$\hat{L}_1=0.35$	$\hat{L}_1=0.375$	$\hat{L}_1=0.4$
$\frac{\partial \hat{F}}{\partial \hat{L}_1}$	0.031	0.031	0.031		0.68	0.68	0.68
	$\hat{w}=0.027$	$\hat{w}=0.03$	$\hat{w}=0.033$		$\hat{w}=0.225$	$\hat{w}=0.25$	$\hat{w}=0.275$
$\frac{\partial \hat{F}}{\partial \hat{w}}$	0.012	0.016	0.019		0.256	0.34	0.431

Table 3-6. Sensitivity coefficients of force for $\hat{\delta}$, $\hat{L}_1$ and $\hat{w}$ at sliding velocity $\hat{U}=-10$. Nominal conditions given by Equations (3.1) and (3.2).

Now the sensitivity plots for force are shown for varying sliding velocities in Figures 3-9 through 3-26 where parameters $\hat{L}_1$, $\hat{\delta}$ and $\hat{w}$ are plotted against $\hat{L}_1$, $\hat{\delta}$ and $\hat{w}$ individually for the nominal conditions. The discussion of these plots will be done in the further sections of the chapter.

Case 1: Short width, $\hat{U}=10$. Nominal conditions $\hat{\delta}=40;\hat{w}=0.03;\hat{L}_1=0.485$.

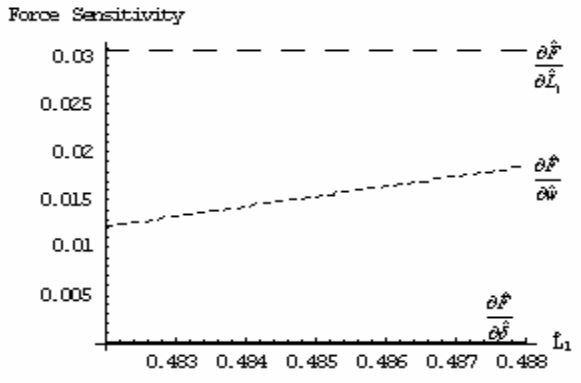

Figure 3-9. Force sensitivities for parameters $\hat{L}_1$, $\hat{\delta}$ and $\hat{w}$ along length $\hat{L}_1$.

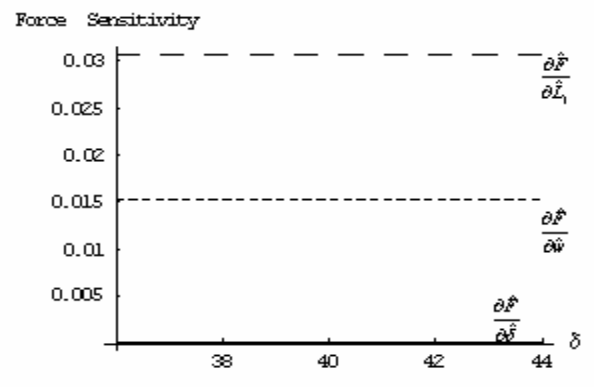

Figure 3-10. Force sensitivities for parameters $\hat{L}_1$, $\hat{\delta}$ and $\hat{w}$ along depth $\hat{\delta}$.

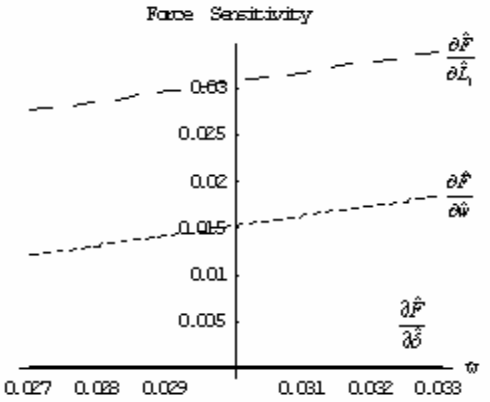

Figure 3-11. Force sensitivities for parameters $\hat{L}_1$, $\hat{\delta}$ and $\hat{w}$ along width $\hat{w}$.

Case 2: Long width, $\hat{U} = 10$. Nominal conditions $\hat{\delta} = 1; \hat{w} = 0.25; \hat{L}_1 = 0.375$.

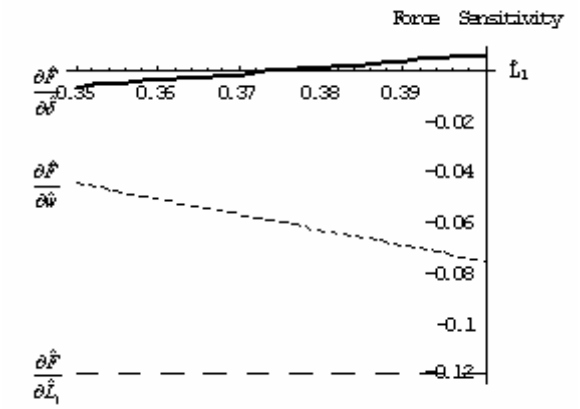

Figure 3-12. Force sensitivities for parameters $\hat{L}_1$, $\hat{\delta}$ and $\hat{w}$ along length $\hat{L}_1$.

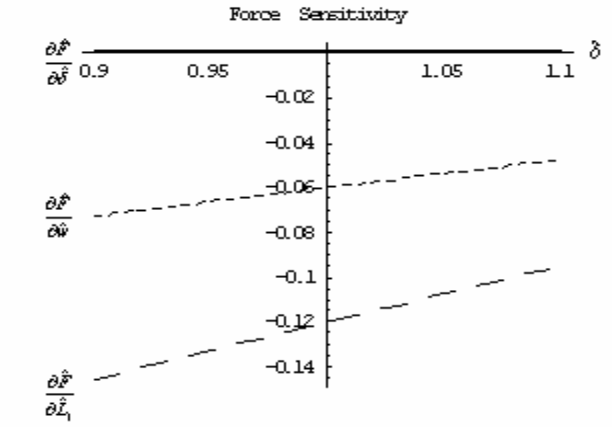

Figure 3-13. Force sensitivities for parameters $\hat{L}_1$, $\hat{\delta}$ and $\hat{w}$ along depth $\hat{\delta}$.

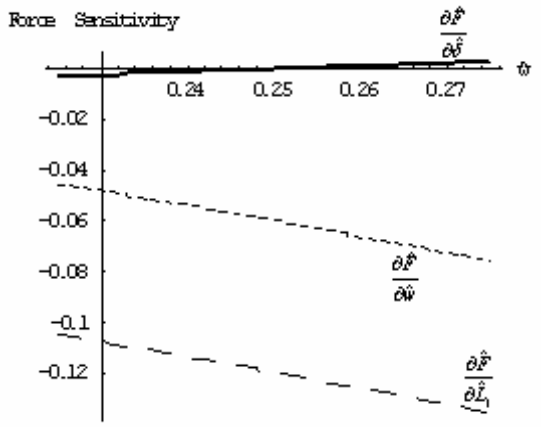

Figure 3-14. Force sensitivities for parameters $\hat{L}_1$, $\hat{\delta}$ and $\hat{w}$ along width $\hat{w}$.

Case 3: Short width, $\hat{U} = 0$. Nominal conditions $\hat{\delta} = 40; \hat{w} = 0.03; \hat{L}_1 = 0.485$.

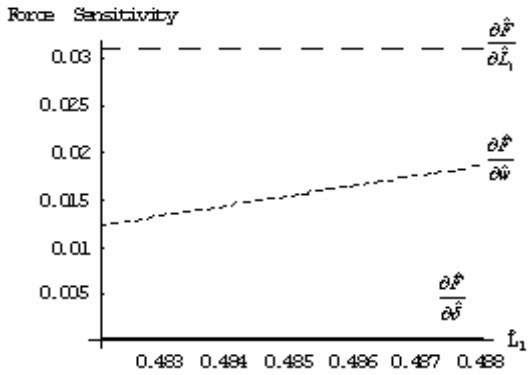

Figure 3-15. Force sensitivities for parameters $\hat{L}_1$, $\hat{\delta}$ and $\hat{w}$ along length $\hat{L}_1$.

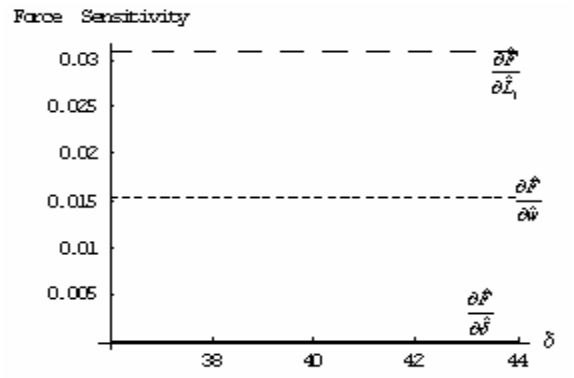

Figure 3-16. Force sensitivities for parameters $\hat{L}_1$, $\hat{\delta}$ and $\hat{w}$ along depth $\hat{\delta}$.

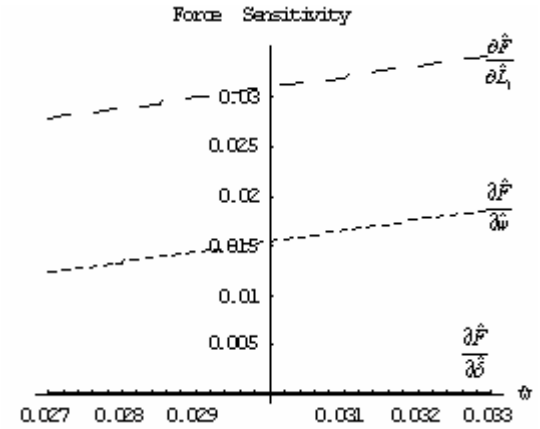

Figure 3-17. Force sensitivities for parameters $\hat{L}_1$, $\hat{\delta}$ and $\hat{w}$ along width $\hat{w}$.

Case 4: Long width, $\hat{U} = 0$. Nominal conditions $\hat{\delta} = 1; \hat{w} = 0.25; \hat{L}_1 = 0.375$.

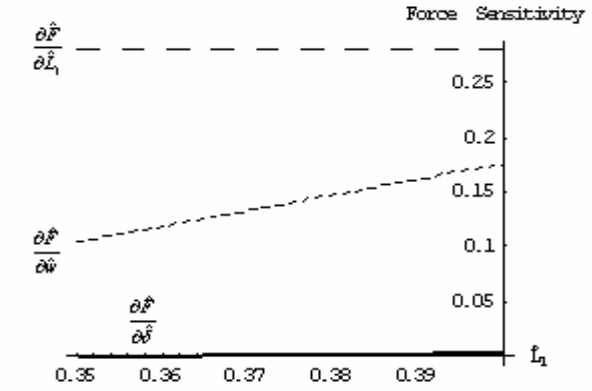

Figure 3-18. Force sensitivities for parameters $\hat{L}_1$, $\hat{\delta}$ and $\hat{w}$ along length $\hat{L}_1$.

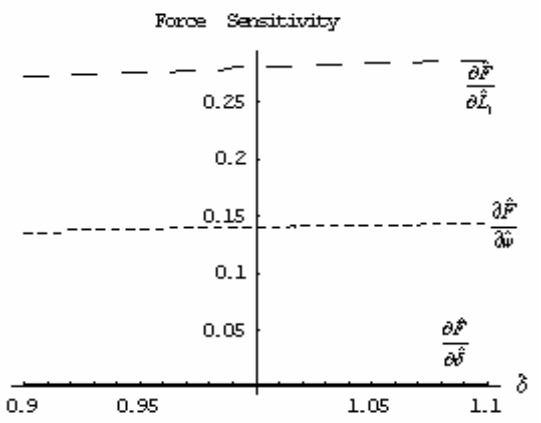

Figure 3-19. Force sensitivities for parameters $\hat{L}_1$, $\hat{\delta}$ and $\hat{w}$ along depth $\hat{\delta}$.

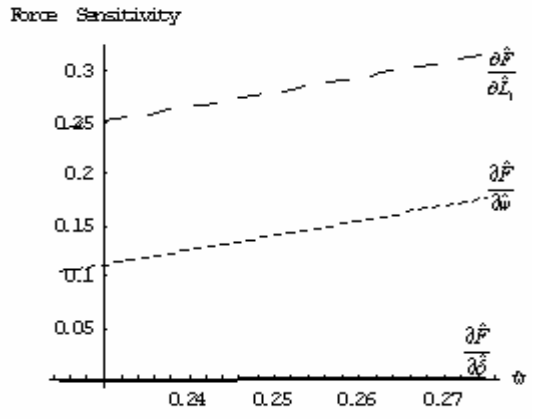

Figure 3-20. Force sensitivities for parameters $\hat{L}_1$, $\hat{\delta}$ and $\hat{w}$ along width $\hat{w}$.

Case 5: Short width, $\hat{U} = -10$. Nominal conditions $\hat{\delta} = 40; \hat{w} = 0.03; \hat{L}_1 = 0.485$.

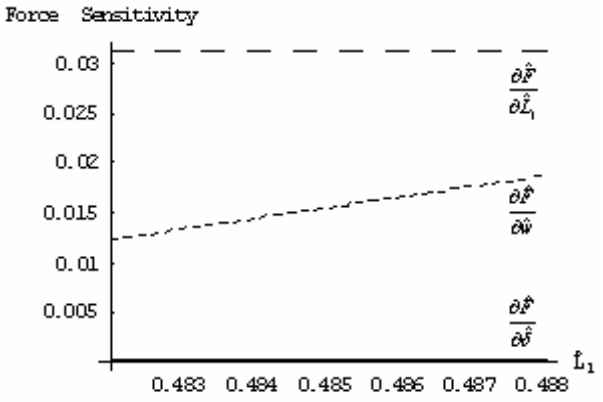

Figure 3-21. Force sensitivities for parameters $\hat{L}_1$, $\hat{\delta}$ and $\hat{w}$ along length $\hat{L}_1$.

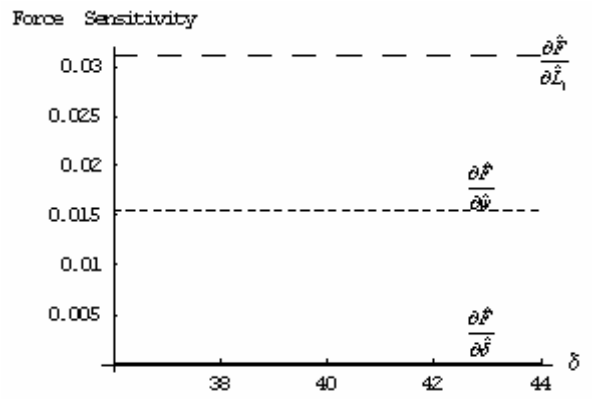

Figure 3-22. Force sensitivities for parameters $\hat{L}_1$, $\hat{\delta}$ and $\hat{w}$ along depth $\hat{\delta}$.

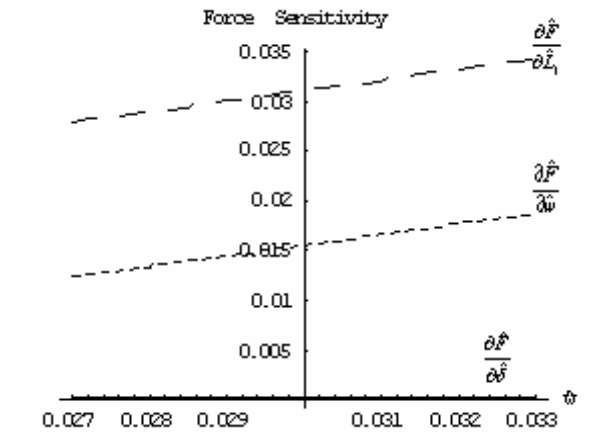

Figure 3-23. Force sensitivities for parameters $\hat{L}_1$, $\hat{\delta}$ and $\hat{w}$ along width $\hat{w}$.

Case 6: Long width, $\hat{U} = -10$. Nominal conditions $\hat{\delta} = 1; \hat{w} = 0.25; \hat{L}_1 = 0.375$.

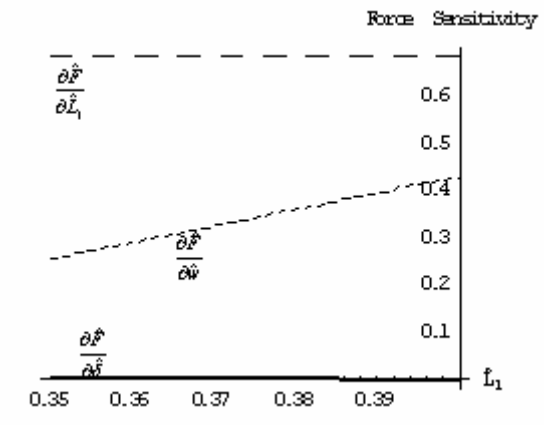

Figure 3-24. Force sensitivities for parameters $\hat{L}_1$, $\hat{\delta}$ and $\hat{w}$ along length $\hat{L}_1$.

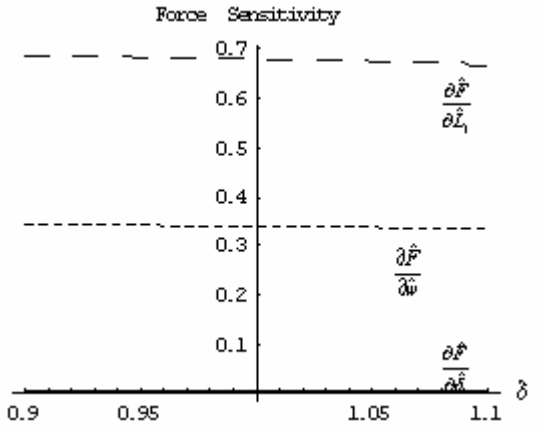

Figure 3-25. Force sensitivities for parameters $\hat{L}_1$, $\hat{\delta}$ and $\hat{w}$ along depth $\hat{\delta}$.

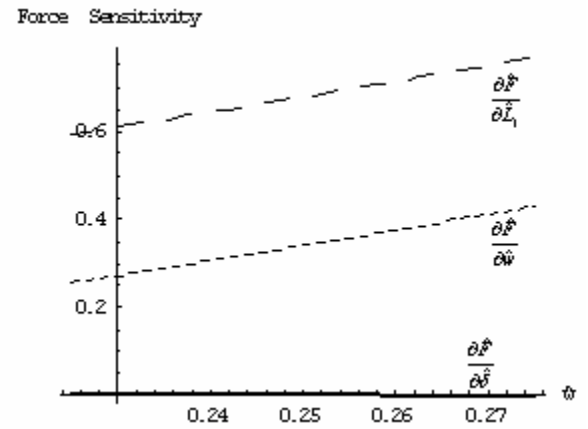

Figure 3-26. Force sensitivities for parameters $\hat{L}_1$, $\hat{\delta}$ and $\hat{w}$ along width $\hat{w}$.

3.4.2 Discussion for Force Sensitivity with Respect to Length

Consider the force sensitivity with respect to length $\hat{L}_1$ given by Equation (3.8). Tables 3-4 through 3-6 show that the magnitude of this force sensitivity is higher in all the cases for all sliding velocities. Also a look into the plots shown in Figures 3-9 thorough 3-26 validates this point and thus it can be concluded that for effective force sensitivity control, the most important quantity is length $\hat{L}_1$ compared to other parameters.

An interesting feature in Table 3-4 is the change of force sensitivity value with respect to the length $\hat{L}_1$ from positive to negative, when the groove geometry changes from short to long width for sliding velocity $\hat{U} = 10$. A look into Equation (3.8) shows that the quantity $R - \hat{U}$ changes its sign based on change in value of groove depth from short width to long width. Also a clearer understanding of this change in force sensitivity sign is shown in Figure 3-27, which shows this gradual transition from a positive force sensitivity value to a negative value. Looking at Equation (3.8), it shows that force sensitivity is depending on two parameters $\hat{w}$ and $\hat{\delta}$. Thus varying these two parameters with respect to their nominal conditions given in Equation (3.1) and (3.2), Figure 3-27 is obtained which clearly indicates the change of force sensitivity sign for variation from short groove width to long width geometry.

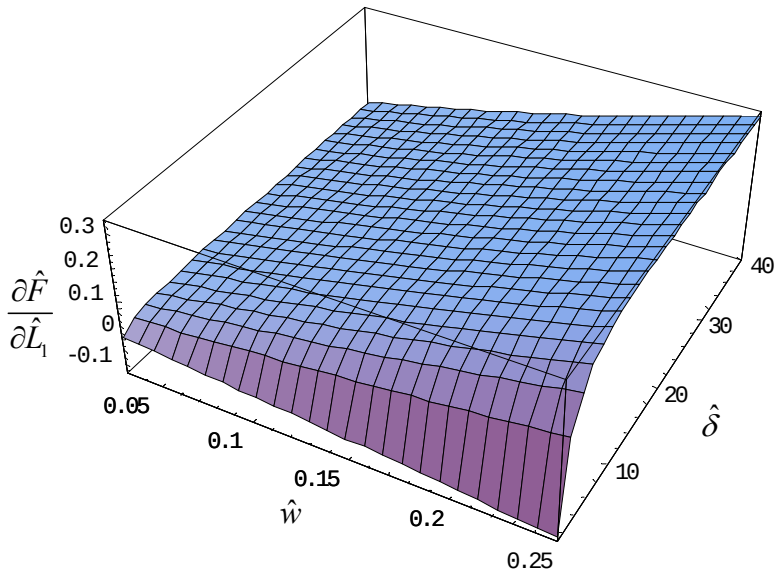

Figure 3-27. 3D plot of variation of force sensitivity $\frac{\partial \hat{F}}{\partial \hat{L}_1}$ for changes of groove width $\hat{w}$ and depth $\hat{\delta}$ from short to long groove geometry, $\hat{U} = 10$.

3.4.3 Discussion for Force Sensitivity with Respect to Groove Width

This section analyzes the influence of groove width on force sensitivity. Consider the force sensitivity with respect to width $\hat{w}$ given by Equation (3.9). Its magnitude shown in Tables 3.4 through 3.6 indicates that this parameter has some influence on the force sensitivity but not as much compared to the parameter $\hat{L}_1$. The Figures 3-9 through 3-26 show that the plot lines fall in between the sensitivity coefficients with respect to $\hat{L}_1$ and $\hat{\delta}$ which shows that groove width is also one of the parameters to be considered for force sensitivity control.

Analyzing Equation (3.9), it is clear that the factor for change in sensitivity sign as seen in Table 3-4 is the quantity $R-\hat{U}$, and the reasoning as explained in the previous section. It could also be explained by looking at the figure below.

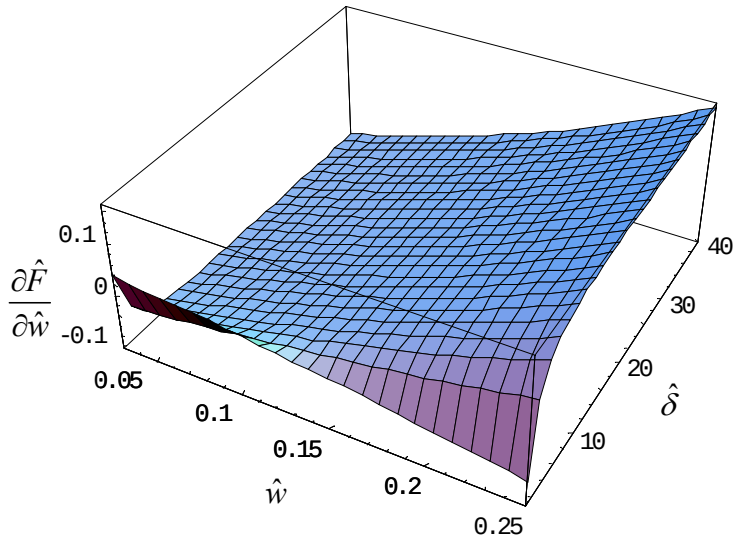

Figure 3-28. 3D plot of variation of force sensitivity $\frac{\partial \hat{F}}{\partial \hat{w}}$ for changes of groove width $\hat{w}$ and depth $\hat{\delta}$ from short to long groove geometry, length $\hat{L}_1 = 0.375$ is constant, $\hat{U} = 10$.

Force sensitivity in Equation (3.9) shows that it depends on three parameters $\hat{L}_1$, $\hat{w}$ and $\hat{\delta}$ and thus to plot a 3D figure to show the force sensitivity $\frac{\partial \hat{F}}{\partial \hat{w}}$ variation, one of the parameters has to be kept constant. Here length $\hat{L}_1$ is kept constant and the other two parameters are varied along the same nominal conditions. The results are shown in Figure 3-28 with the same explanation as for force sensitivity $\frac{\partial \hat{F}}{\partial \hat{L}_1}$. The figures are shown only for the force sensitivity cases but can also be shown for torque sensitivity as well, if there is a change in its sensitivity sign from once case to the other.

3.4.4 Discussion for Force Sensitivity with Respect to Groove Depth

Consider the force sensitivity equation with respect to groove depth $\hat{\delta}$ given by the Equation (3.10). An analysis of this sensitivity from the Tables 3-4 through 3-6 shows that its value is very small compared to other parameters. Also it can be seen that since the value was so low for long groove width cases, its value could not be plotted for all the sliding velocities. The importance of groove depth in force sensitivity can also be clearly understood by looking at the plots in Figures 3-9 through 3-26, where it is seen that this sensitivity is on the zero coordinate axis for almost all groove geometries as well as sliding velocity cases. This indicates that having any groove depth has little or no influence on force sensitivity and that it can be safely neglected during this analysis.

3.5 Torque Sensitivity

Considering the torque sensitivity coefficients now, the sensitivity equations with respect to its influencing parameters were analyzed in Chapter 2 and shown here again.

$$\hat{T} = \frac{\hat{U}\hat{w}\hat{\delta}\left[1-(3\hat{L}_1^{\,2}+3\hat{L}_1\hat{w}+\hat{w}^2)\right]+2(1+\hat{\delta})^3+\hat{w}\hat{\delta}R\left[(3\hat{L}_1^{\,2}+3\hat{L}_1\hat{w}+\hat{w}^2)-3\right]}{6\left[(1+\hat{\delta})^3-\hat{w}\hat{\delta}R\right]} \quad (3.11)$$

$$\frac{\partial \hat{T}}{\partial \hat{L}_1} = -\frac{\hat{w}\hat{\delta}(R-\hat{U})(2\hat{L}_1+\hat{w})}{-2+2(\hat{w}-1)\hat{\delta}R} \quad (3.12)$$

$$\frac{\partial \hat{T}}{\partial \hat{w}} = \frac{\hat{\delta}(R-\hat{U})\left[(1+\hat{\delta})^3(3\hat{L}_1^{\,2}+3\hat{w}^2-1)-2\hat{w}^3\hat{\delta}R-3\hat{L}_1\hat{w}\left((\hat{w}-2)\hat{\delta}R-2\right)\right]}{6\left[\hat{\delta}R(\hat{w}-1)-1\right]^2} \quad (3.13)$$

$$\frac{\partial \hat{T}}{\partial \hat{\delta}} = -\frac{\hat{w}\left(3\hat{L}_1(\hat{L}_1+\hat{w})+\hat{w}^2-1\right)\left[-3(1+\hat{\delta})^2+\hat{U}\left(1+(\hat{w}-1)\hat{\delta}^2(3+2\hat{\delta})\right)\right]}{6\left[\hat{\delta}R(\hat{w}-1)-1\right]^2} \quad (3.14)$$

where R is given by Equation (3.4).

Equations (3.12) through (3.14) show that torque sensitivity depend on $\hat{w},\ \hat{\delta}$ and $\hat{L}_1$.

3.5.1 Torque Results

Substituting the nominal conditions given by Equations (3.1) and (3.2) and their variation into the above equations the results are tabulated and are shown in Table 3-7 through 3-9. The higher the magnitude of the parameter, higher its influence in the operating lubricating condition of the system. The tables are plotted for torque sensitivities with respect to quantities $\hat{w},\ \hat{\delta}$ and $\hat{L}_1$ for short and long groove width geometries and for varying sliding velocity $\hat{U}$ at $10,\ 0, -10$. The results obtained from the table will be discussed in the coming sections.

It can be seen from the tables below that the torque sensitivity for $\hat{L}_1$ and $\hat{w}$ have almost the same values for all short width cases at different sliding velocities, which indicates that these torque sensitivities are independent of sliding velocity.

	SHORT WIDTH $\hat{U}=10$				LONG WIDTH $\hat{U}=10$		
	$\hat{\delta}=36$	$\hat{\delta}=40$	$\hat{\delta}=44$		$\hat{\delta}=0.9$	$\hat{\delta}=1$	$\hat{\delta}=1.1$
$\frac{\partial \hat{T}}{\partial \hat{\delta}}$	-4.90E-07	-3.60E-07	-2.70E-07		-1.00E-02	-9.80E-03	-9.50E-03
	$\hat{L}_1=0.482$	$\hat{L}_1=0.485$	$\hat{L}_1=0.488$		$\hat{L}_1=0.35$	$\hat{L}_1=0.375$	$\hat{L}_1=0.4$
$\frac{\partial \hat{T}}{\partial \hat{L}_1}$	0.015	0.015	0.015		-0.057	-0.06	-0.063
	$\hat{w}=0.027$	$\hat{w}=0.03$	$\hat{w}=0.033$		$\hat{w}=0.225$	$\hat{w}=0.25$	$\hat{w}=0.275$
$\frac{\partial \hat{T}}{\partial \hat{w}}$	-0.038	-0.037	-0.035		-9.90E-04	-8.50E-03	-1.70E-02

Table 3-7. Sensitivity coefficients of torque for $\hat{\delta}$, $\hat{L}_1$ and $\hat{w}$ at sliding velocity $\hat{U}=10$. Nominal conditions given by Equations (3.1) and (3.2).

	SHORT WIDTH $\hat{U}=0$				LONG WIDTH $\hat{U}=0$		
	$\hat{\delta}=36$	$\hat{\delta}=40$	$\hat{\delta}=44$		$\hat{\delta}=0.9$	$\hat{\delta}=1$	$\hat{\delta}=1.1$
$\frac{\partial \hat{T}}{\partial \hat{\delta}}$	-2.10E-09	-1.40E-09	-9.70E-10		-3.60E-03	-3.00E-03	-2.50E-03
	$\hat{L}_1=0.482$	$\hat{L}_1=0.485$	$\hat{L}_1=0.488$		$\hat{L}_1=0.35$	$\hat{L}_1=0.375$	$\hat{L}_1=0.4$
$\frac{\partial \hat{T}}{\partial \hat{L}_1}$	0.015	0.015	0.015		0.133	0.14	0.147
	$\hat{w}=0.027$	$\hat{w}=0.03$	$\hat{w}=0.033$		$\hat{w}=0.225$	$\hat{w}=0.25$	$\hat{w}=0.275$
$\frac{\partial \hat{T}}{\partial \hat{w}}$	-0.038	-0.036	-0.035		2.30E-03	1.98E-02	3.96E-02

Table 3-8. Sensitivity coefficients of torque for $\hat{\delta}$, $\hat{L}_1$ and $\hat{w}$ at sliding velocity $\hat{U}=0$. Nominal conditions given by Equations (3.1) and (3.2).

	SHORT WIDTH $\hat{U}=-10$				LONG WIDTH $\hat{U}=-10$		
	$\hat{\delta}=36$	$\hat{\delta}=40$	$\hat{\delta}=44$		$\hat{\delta}=0.9$	$\hat{\delta}=1$	$\hat{\delta}=1.1$
$\frac{\partial \hat{T}}{\partial \hat{\delta}}$	4.90E-07	3.60E-07	2.70E-07		2.80E-03	3.90E-03	4.50E-03
	$\hat{L}_1=0.482$	$\hat{L}_1=0.485$	$\hat{L}_1=0.488$		$\hat{L}_1=0.35$	$\hat{L}_1=0.375$	$\hat{L}_1=0.4$
$\frac{\partial \hat{T}}{\partial \hat{L}_1}$	0.016	0.016	0.016		0.323	0.34	0.357
	$\hat{w}=0.027$	$\hat{w}=0.03$	$\hat{w}=0.033$		$\hat{w}=0.225$	$\hat{w}=0.25$	$\hat{w}=0.275$
$\frac{\partial \hat{T}}{\partial \hat{w}}$	-0.038	-0.037	-0.035		5.60E-03	4.80E-02	9.60E-02

Table 3-9. Sensitivity coefficients of torque for $\hat{\delta}$, $\hat{L}_1$ and $\hat{w}$ at sliding velocity $\hat{U}=-10$. Nominal conditions given by Equations (3.1) and (3.2).

Sensitivity plots for torque are shown below for varying sliding velocities where parameters $\hat{L}_1$, $\hat{\delta}$ and $\hat{w}$ are plotted against $\hat{L}_1$, $\hat{\delta}$ and $\hat{w}$ individually for the nominal conditions given.

Case 1: Short width, $\hat{U}=10$. Nominal conditions $\hat{\delta}=40; \hat{w}=0.03; \hat{L}_1=0.485$

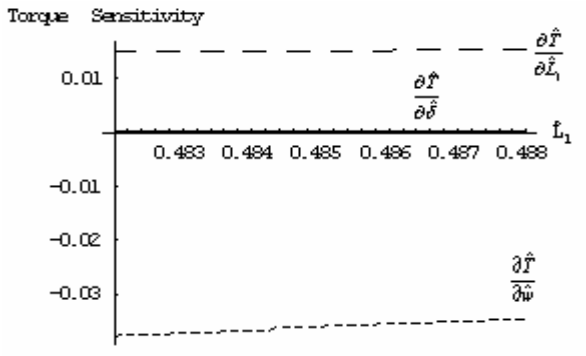

Figure 3-29. Torque sensitivities for parameters $\hat{L}_1$, $\hat{\delta}$ and $\hat{w}$ along length $\hat{L}_1$.

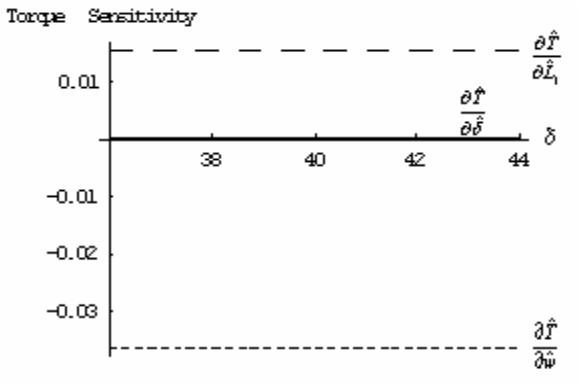

Figure 3-30. Torque sensitivities for parameters $\hat{L}_1$, $\hat{\delta}$ and $\hat{w}$ along depth $\hat{\delta}$.

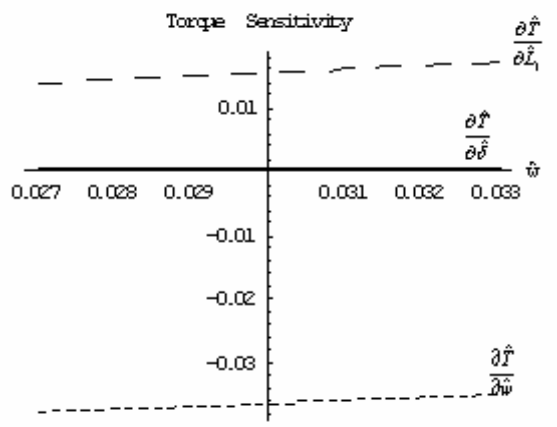

Figure 3-31. Torque sensitivities for parameters $\hat{L}_1$, $\hat{\delta}$ and $\hat{w}$ along width $\hat{w}$.

Case 2: Long width, $\hat{U} = 10$. Nominal conditions $\hat{\delta} = 1; \hat{w} = 0.25; \hat{L}_1 = 0.375$

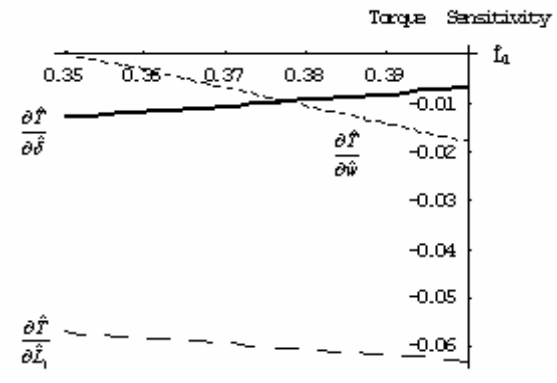

Figure 3-32. Torque sensitivities for parameters $\hat{L}_1$, $\hat{\delta}$ and $\hat{w}$ along length $\hat{L}_1$.

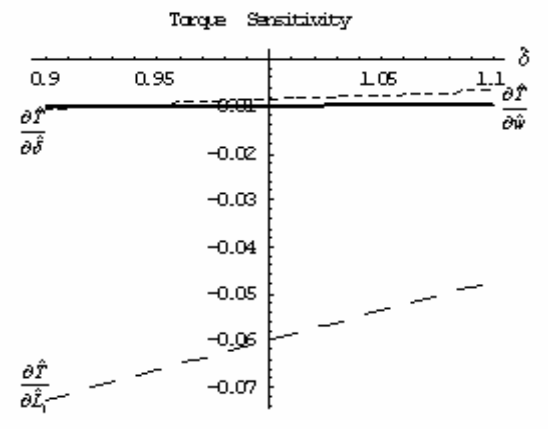

Figure 3-33. Torque sensitivities for parameters $\hat{L}_1$, $\hat{\delta}$ and $\hat{w}$ along depth $\hat{\delta}$.

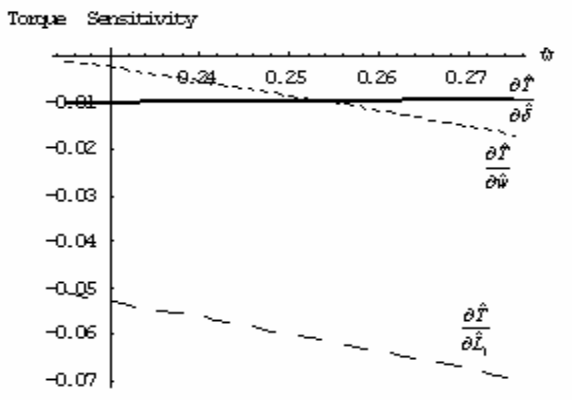

Figure 3-34. Torque sensitivities for parameters $\hat{L}_1$, $\hat{\delta}$ and $\hat{w}$ along width $\hat{w}$.

Case 3: Short width, $\hat{U} = 0$. Nominal conditions $\hat{\delta} = 40; \hat{w} = 0.03; \hat{L}_1 = 0.485$

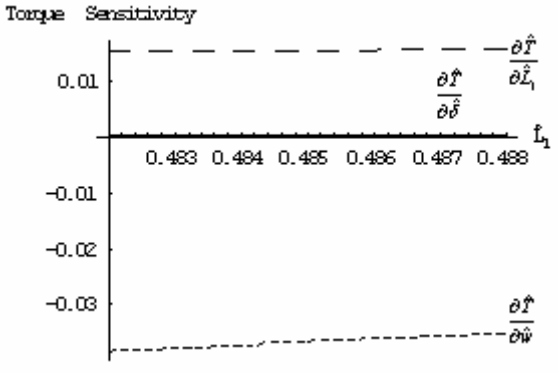

Figure 3-35. Torque sensitivities for parameters $\hat{L}_1$, $\hat{\delta}$ and $\hat{w}$ along length $\hat{L}_1$.

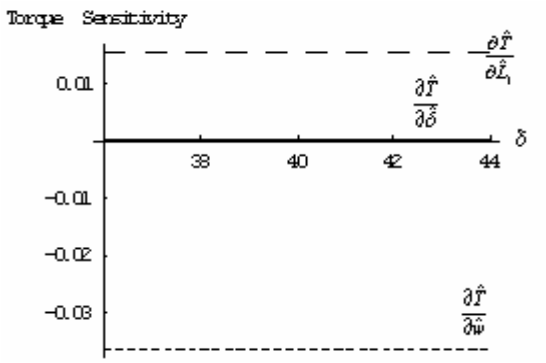

Figure 3-36. Torque sensitivities for parameters $\hat{L}_1$, $\hat{\delta}$ and $\hat{w}$ along depth $\hat{\delta}$.

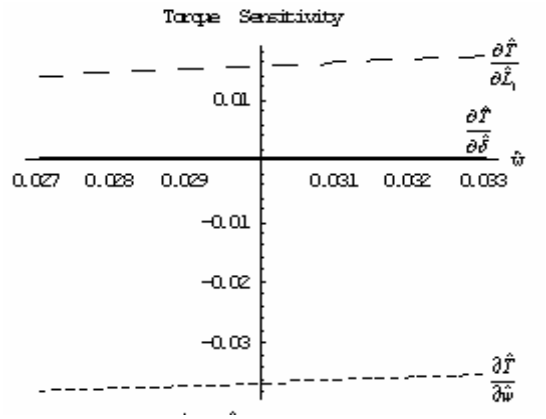

Figure 3-37. Torque sensitivities for parameters $\hat{L}_1$, $\hat{\delta}$ and $\hat{w}$ along width $\hat{w}$.

Case 4: Long width, $\hat{U} = 0$. Nominal conditions $\hat{\delta} = 1; \hat{w} = 0.25; \hat{L}_1 = 0.375$

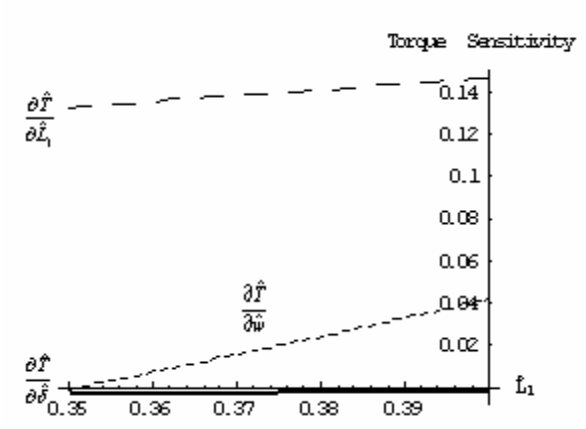

Figure 3-38. Torque sensitivities for parameters $\hat{L}_1$, $\hat{\delta}$ and $\hat{w}$ along length $\hat{L}_1$.

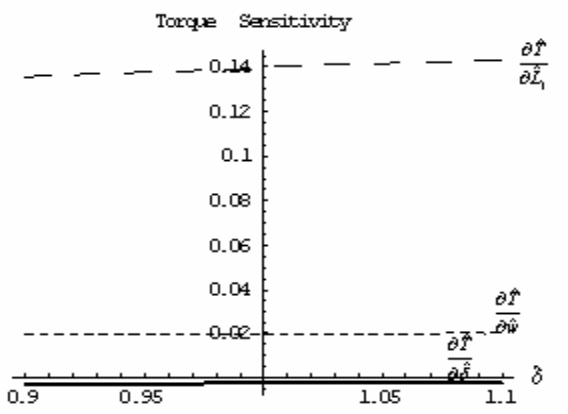

Figure 3-39. Torque sensitivities for parameters $\hat{L}_1$, $\hat{\delta}$ and $\hat{w}$ along depth $\hat{\delta}$.

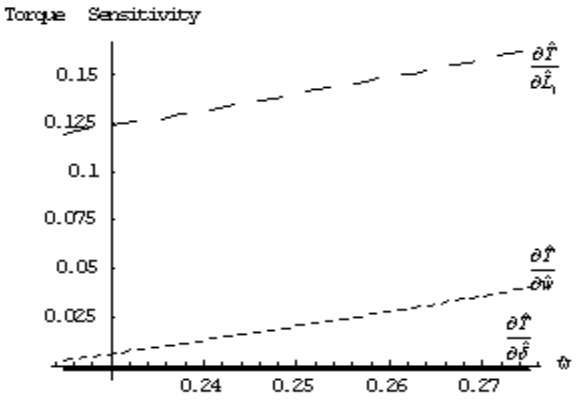

Figure 3-40. Torque sensitivities for parameters $\hat{L}_1$, $\hat{\delta}$ and $\hat{w}$ along width $\hat{w}$.

Case 5: Short width, $\hat{U} = -10$. Nominal conditions $\hat{\delta} = 40; \hat{w} = 0.03; \hat{L}_1 = 0.485$

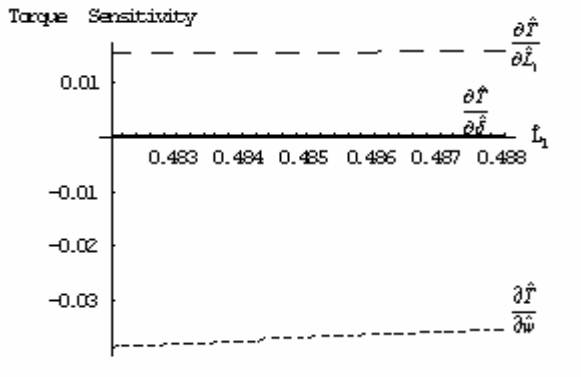

Figure 3-41. Torque sensitivities for parameters $\hat{L}_1$, $\hat{\delta}$ and $\hat{w}$ along length $\hat{L}_1$.

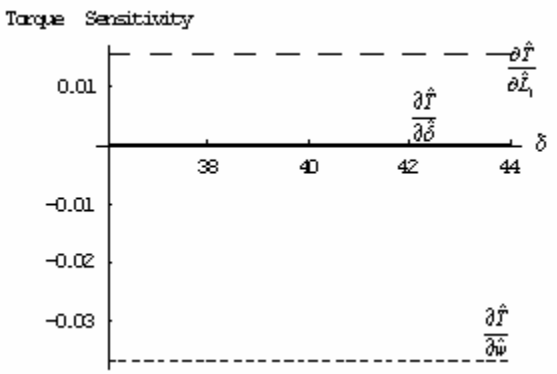

Figure 3-42. Torque sensitivities for parameters $\hat{L}_1$, $\hat{\delta}$ and $\hat{w}$ along depth $\hat{\delta}$.

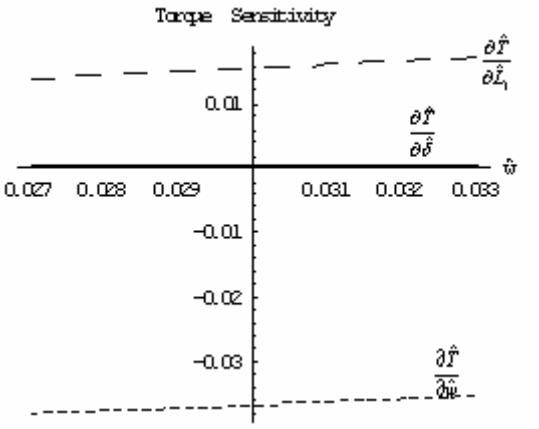

Figure 3-43. Torque sensitivities for parameters $\hat{L}_1$, $\hat{\delta}$ and $\hat{w}$ along width $\hat{w}$.

Case 6: Long width, $\hat{U} = -10$. Nominal conditions $\hat{\delta} = 1; \hat{w} = 0.25; \hat{L}_1 = 0.375$

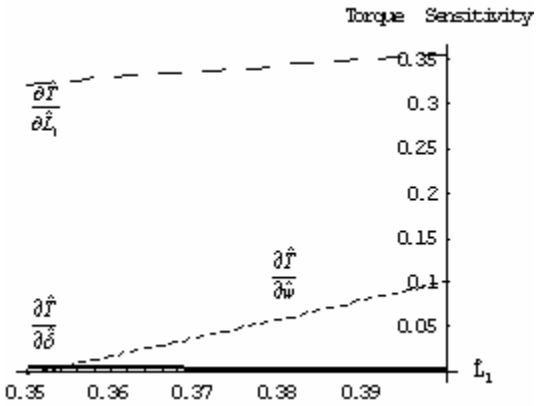

Figure 3-44. Torque sensitivities for parameters $\hat{L}_1$, $\hat{\delta}$ and $\hat{w}$ along length $\hat{L}_1$.

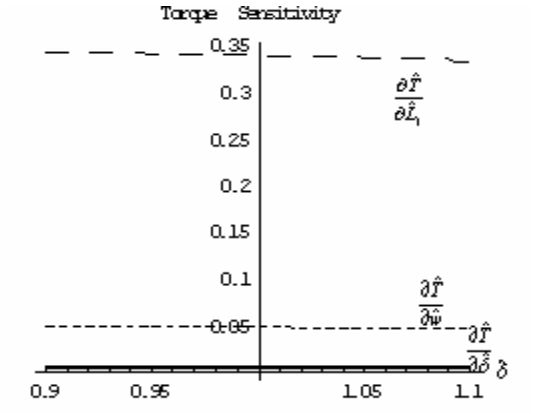

Figure 3-45. Torque sensitivities for parameters $\hat{L}_1$, $\hat{\delta}$ and $\hat{w}$ along depth $\hat{\delta}$.

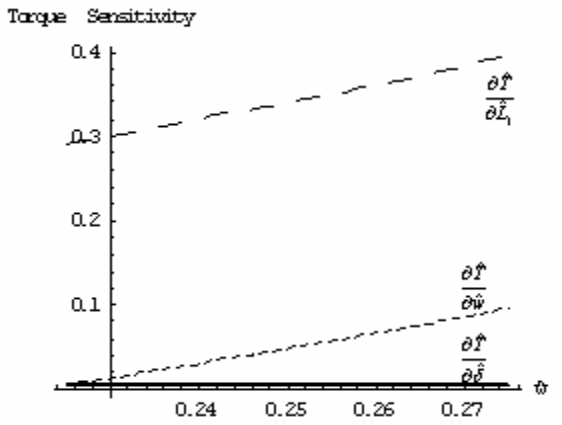

Figure 3-46. Torque sensitivities for parameters $\hat{L}_1$, $\hat{\delta}$ and $\hat{w}$ along width $\hat{w}$.

3.5.2 Discussion for Torque Sensitivity with Respect to Length

Consider the torque sensitivity with respect to length $\hat{L}_1$ given by Equation (3.12). Its sensitivity values have been plotted in Tables 3-7 through 3-9 and it can be seen that for short groove widths, it magnitude is less compared to torque sensitivity $\frac{\partial \hat{T}}{\partial \hat{w}}$ whereas its magnitude is the highest for long groove width geometries. This indicates that

parameter $\hat{L}_1$ is more influential in torque sensitivity control for long groove widths. Figures 3-32 through 3-34, 3-38 through 3-40 and 3-44 through 3-46 clearly show the importance of length $\hat{L}_1$ as the most influencing parameter in torque sensitivity control. Also the plots for short groove widths are almost a straight line, which indicates that sensitivities don't change much for nominal condition variation.

As was the similar case in force sensitivity, it can be seen in Table 3-7, that the sign for $\frac{\partial \hat{T}}{\partial \hat{L}_1}$ changes from positive to negative for the change of groove geometry and the explanation for this can be given from the Equation (3.12). The denominator is always negative because of the quantity $\hat{w}-1$ being less than zero, thus rendering the whole sensitivity term positive. So the only influencing factor for the change of sign is the quantity $R-\hat{U}$. Thus when the groove width changes from short to long, the value of $\hat{\delta}$ changes from 40 to 1 resulting in $R-\hat{U}$ being negative, where $\hat{U}$ is positive. Other sensitivity sign changes in the tables can be explained in the similar manner.

3.5.3 Discussion for Torque Sensitivity with Respect to Groove width

This section analyzes the influence of groove width $\hat{w}$ on torque sensitivity and its values are shown in Tables 3-7 through 3-9. The higher magnitude numbers for short groove widths clearly indicate that groove width is more influential for these groove geometries compared to long groove widths where sensitivity $\frac{\partial \hat{T}}{\partial \hat{L}_1}$ has a better influence. Figures 3-29 through 3-31, 3-35 through 3-37 and 3-41 through 3-43 prove the above

conclusion. The other plots indicate that $\frac{\partial \hat{T}}{\partial \hat{w}}$ varies linearly for changes in nominal condition and is more influential than torque sensitivity with respect to groove depth $\hat{\delta}$.

There is a change in torque sensitivity sign with respect to groove width as observed in Tables 3-8 and 3-9. As seen in the previous sections, the quantity that changed the sensitivity sign was $R-\hat{U}$. For long groove widths $R-\hat{U}$ returns a negative values for sliding velocity 10 and positive values for sliding velocity 0 and –10. Thus the force sensitivity values for long widths are negative in Table 3-7 and are positive in Tables 3-8 and 3-9.

3.5.4 Discussion for Torque Sensitivity with Respect to Groove Depth

Lastly consider the equation of sensitivity coefficient $\frac{\partial \hat{T}}{\partial \hat{\delta}}$, which is given by the Equation (3.14). For almost all the groove geometries cases at different sliding velocities, the magnitude of this sensitivity is very low as seen in Tables 3-7 through 3-9. This clearly states that the effect of groove depth is minimal in torque sensitivity. Figures 3-29 through 3-31, 3-35 through 3-37 and 3-41 through 3-43 show that the sensitivity values are along the zero coordinate axis for short groove widths and for long groove geometries, its magnitude is very small. Thus it can be concluded from these results that groove depth $\hat{\delta}$ can be safely neglected during torque sensitivity analysis.

3.6 Conclusion

This chapter analyzed the flow rate, force and torque sensitivities effecting the lubrication of the flat plate system and the results were tabulated and also plotted. Two

cases of the flat plate system for analysis were considered: A short groove width and a long groove width. The resulting tables as well as the plots gave an insight into the individual significance of the system parameters $\hat{L}_1$, $\hat{\delta}$ and $\hat{w}$. The analysis of flow rate sensitivity has shown that it is independent of the effects of length $\hat{L}_1$. Force and torque sensitivity analysis has shown that for effective control of the flat plate system, the parameter of influence depends on the groove width geometry and that groove depth could be neglected. These results were analyzed and suitable assumptions that influence lubrication are made which is shown in the following conclusion chapter.

CHAPTER 4. CONCLUSION AND FUTURE WORK

In this chapter, conclusions that are based and supported by the results and discussion of Chapter 3, considering the sensitivity of flow, force and torque for the two cases of short and long width grooves and their effects on the lubrication of the flat plate system because of parameters $\hat{L}_1$, $\hat{\delta}$ and $\hat{w}$ are listed. Possible future work that could be carried out after this project is also listed.

4.1 Conclusions

The governing equations for the results are given by Equations (3.5) and (3.6), (3.8) through (3.10) and (3.12) through (3.14) in Chapter 3. These equations are used to tabulate the sensitivity values and plots shown in Tables 3-1 through 3-9 and Figures 3-3 through 3-46 respectively. Valuable conclusions can be made based on the information obtained from these tables and plots.

4.1.1 Flow Sensitivity Conclusions

1. Flow rate sensitivity is independent of length $\hat{L}_1$ as seen from Equations (3.5) and (3.6) in Chapter 3. This implies that the groove can be placed anywhere along the length of the *x*-axis of the flat plate system without having any effect on flow rate sensitivity.
2. Sensitivities do not change much with parameter variation for short groove width geometries as shown in Figures 3-3 through 3-5 and flow sensitivities change with parameter variation as indicated by Figures 3-6 through 3-8 in Chapter 3.

3. Groove width $\hat{w}$ is the most influencing parameter in flow rate sensitivity. The magnitude of flow sensitivity with respect to groove depth $\hat{\delta}$ was seen to be very low, which concludes that this quantity can be neglected during the sensitivity analysis.
4. Sliding velocity $\hat{U}$ has no effect on flow rate sensitivity for short width deep groove geometry cases.

4.1.2 Force Sensitivity Conclusions

1. Length $\hat{L}_1$ has the highest impact on force sensitivity followed by groove width $\hat{w}$. This is clearly seen in Figures 3-9 through 3-26.
2. The force sensitivity with respect to groove depth $\hat{\delta}$ have a very low magnitude and follow the zero axis line when plotted, which indicates that groove depth has little or no effect and that it can be in neglected in force sensitivity analysis.

4.1.3 Torque Sensitivity Conclusions

1. Torque sensitivities with respect to parameters $\hat{L}_1$ and $\hat{w}$ for short width geometries are independent of sliding velocity $\hat{U}$.
2. Length $\hat{L}_1$ is more influential for long groove widths whereas groove width $\hat{w}$ is more important for short groove widths.
3. For short groove widths, torque sensitivity with respect to length $\hat{L}_1$ do not change much for nominal condition variation i.e. it's almost a straight line.

4. Torque sensitivity with respect to groove depth $\hat{\delta}$ has low magnitude for all cases and thus is of minimal importance and can be neglected during this analysis.

4.2 Scope for future work

The analysis done during this project gives some important results for the lubrication groove in hydraulic machinery and valuable conclusions have been drawn from it. However there is also scope for some future work that could be carried out to further validate our results conclusively. Some of the suggestions are:

1. The basis of the analysis, results and conclusions obtained in this project is on theoretical calculations. These results could be further validated by real time practical experiments.
2. CFD software has its limitations in the minimum dimension size a system could have. Considering the extreme small gap between the plate and housing, if this limitation is resolved, CFD analysis could also be done to validate the results. One method could be to subprogram the commands in other software like C, C++ and then import and execute these commands in Fluent.
3. The analysis and results conducted in this thesis involved single groove geometry. Analysis could also be done to determine the effect of multiple grooves on lubrication effects in hydraulic machinery.
4. The analysis in this thesis was conducted for a flat plate system and could be extended to a cylindrical geometry, as this is the most common form of geometry currently used in the hydraulic industry.

REFERENCES

Blatter, A., Maillat, M., Pimenov, S. M., Shafeev, G. A., Simakin, A. V. 1998. "Lubricated friction of laser micro-patterned sapphire flats." Tribology Letters. 4: 237-241

Collins, J. A. 2003. Mechanical Design of Machine Elements and Machines. New York: John Wiley and Sons, Inc.

Costa, L., Fillon, M., Miranda, A. S., Claro, J. C. P. 2000. " An Experimental Investigation of the Effect of Groove Location and Supply Pressure on the THD Performance of a Steadily Loaded Journal Bearing." Journal of Tribology. 122: 227-232

Fox, R. W, McDonald, A. T. 1985. Introduction to Fluid Mechanics. New York: John Wiley and Sons, Inc

Hargreaves, D. J., Elgezawy, A. S. 1998. "A New Model for Combined Couette and Poiseuille Flows in the Transverse Groove of a Plane Inclined Slider Bearing." Tribology International. 31: 6: 297-303

Ivantysynova, M., Huang, C. 2002. "Investigation of the Gap Flow in Displacement Machines Considering Elastohydrodynamic Effect." 5th JFPS International Symposium on Fluid Power. Nara, Japan. 219-229.

Lansdown, A. R. 2004. Lubrication and Lubricant Selection. New York: ASME Press

Manring, N. D. 2005. Hydraulic Control Systems. New York: John Wiley and Sons, Inc

Ronen, A., Etsion, I. 2001. "Friction-Reducing Surface-Texturing in Reciprocating Automotive Components." Tribology Transactions. 44: 3: 359-366

Sahlin, F., Glavatskih, S. B., Almqvist, T., Larsson, R. 2005. "Two-Dimensional CFD-Analysis of Micro-Patterned Surfaces in Hydrodynamic Lubrication." Journal of Tribology. 127: 96-102

Yu, T. H., Sadeghi, F. 2001. "Groove Effects on Thrust Washer Lubrication." Journal of Tribology. 123: 295-304

Zhang, H., Mitsuya, Y., Yamada, M. 2003. "Spreading Characteristics of Molecularly Thin Lubricant on Surfaces With Groove-Shaped Textures: Effects of Molecular Weight and End-Group Functionality." Journal of Tribology. 125: 350-357

Zhang, H., Mitsuya, Y., Yamada, M. 2003. "Spreading Characteristics of Molecularly Thin Lubricant on Surfaces With Groove-Shaped Textures: Monte Carlo Simulation and Measurement Using PFPE Film." Journal of Tribology. 124: 575-583